



## **Tolerance Analysis of Assemblies Using Kinematically Derived Sensitivities**

ADCATS Report No. 99-3

Paul J. Faerber, graduate student  
Department of Mechanical Engineering  
Brigham Young University

MS thesis sponsored by ADCATS

August 1999

### **ABSTRACT**

To estimate tolerance accumulation in an assembly requires the calculation of the tolerance sensitivity of critical assembly features to each source of dimensional variation in the assembly. A Root-Sum-Squares expression may then be formulated to predict the variance and percent rejects to expect in production. To analyze accumulation in a mechanism, rather than a static assembly, requires that this procedure be repeated in multiple positions, since the sensitivities change with the position geometry.

An analogy between tolerance analysis and velocity analysis is described which enables the calculation of the sensitivities in closed form using a kinematic model and classical kinematic analysis. The Jacobian matrix of kinematic analysis will be identical to the tolerance sensitivity matrix if the kinematic model is modified to include dimensional variation and if the kinematic variables are defined correctly. Commercial kinematics software may then be used to update the geometry and calculate the tolerance sensitivities in each position.

A set of variational model elements is presented, which may be added to a kinematic model, resulting in an "equivalent variational mechanism" (EVM), which includes dimensional variations as kinematic inputs. Demonstration of this method using the commercially available software ADAMS is presented. As a side benefit, the kinematic software can even analyze static assemblies, which have no moving parts.

## Chapter 1. Introduction

### 1.1 Background Information

Tolerance analysis is a valuable tool which can aid in the reduction of manufacturing costs and improve quality. Computer-aided tolerance analysis, based on tolerance sensitivities, has made this tool available to designers. Many designers also use commercial kinematic packages based on kinematic sensitivities (ratios of the output to the input motion) to determine velocities and accelerations in mechanism. The objective of this thesis is to determine the relationship between the tolerance sensitivities and the kinematic sensitivities, so that kinematic analysis software can be used to perform tolerance analysis of assemblies and mechanisms.

Tolerance variation in mechanisms is dependent on the position of the mechanism. That is, the mechanism will have different tolerance sensitivities for each new position of the mechanism (Figure 1.1). This requires rebuilding and re-analyzing the mechanism for each new position of interest. This process is time-consuming and prone to error.

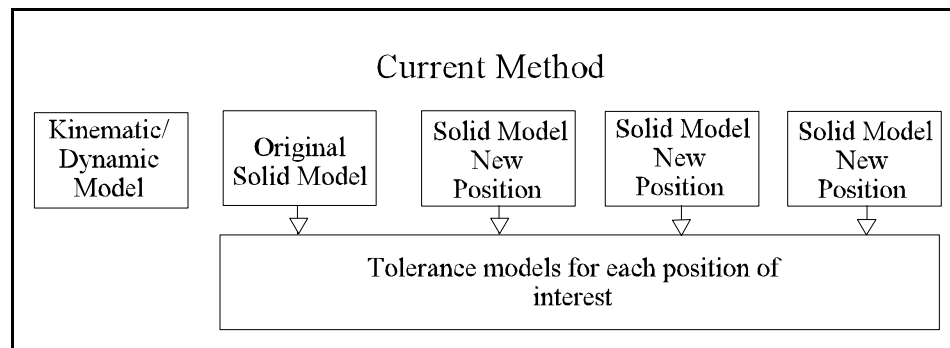


**Figure 1.1** Current techniques used for modeling tolerance and kinematic/dynamic properties of mechanisms.

Ideally, the designer could use the kinematic sensitivities generated by commercial kinematics software for tolerance analysis (Figure 1.2). This would allow the tolerance analysis to be quickly performed for each position of the mechanism, leading to a dynamic tolerance analysis over a full range of motion of a mechanism.

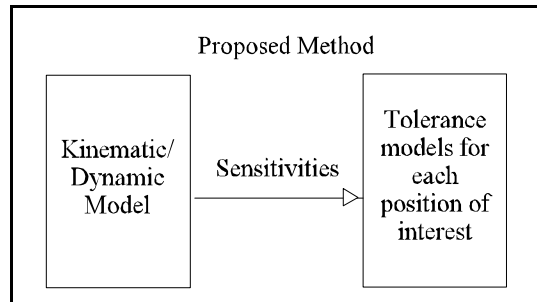


**Figure 1.2** Proposed method for tolerance analysis of mechanisms.

This method would be equally applicable to static assemblies. Many static assemblies have mating conditions between the parts that require a kinematic model to describe the internal adjustments which occur due to dimensional variation. A kinematic modeler would seem ideally suited for this task, except that kinematic models do not account for varying dimensions. An alternative method of calculating tolerance sensitivities provides computer-aided tolerance analysis to designers who don't have access to commercially available tolerance analysis software.

## 1.2 Problem Statement

Differences between the two types of analysis make it difficult to directly use kinematic sensitivities in a tolerance analysis. Kinematic analysis determines output positions and velocities of mechanisms with fixed dimensions. Kinematic analysis calculates sensitivities with respect to position and velocity inputs at joints. Tolerance

analysis determines the output variations of assemblies with dimensions that are allowed to vary. Tolerance sensitivities are calculated with respect to these varying dimensions. So, tolerance analysis describes the variation of one assembly relative to another, while kinematics describes the motion of a single assembly. Relationships between the two types of sensitivities must be established in order to use kinematic sensitivities in tolerance analysis.

### **1.3 Review of Previous Research**

Early research into tolerance sensitivities focuses on problems where dependent variations can be expressed explicitly in terms of the independent variations. Hartenberg and Denavit [9] use closed form expressions to calculate the effect of each independent variation on the total assembly variation by perturbing one design variable at a time. The tolerance sensitivity of each independent variable is the individual variables contribution divided by the total assembly variation. Knappe [11] calculates these sensitivities directly using partial derivatives of the closed form expression describing the assembly.

There are several disadvantages to both methods. Often, explicit expressions are difficult or impossible to develop for mechanisms with any degree of complexity. When these expressions are found, numerical techniques are often required to generative partial derivatives. These two methods work well only for simple assemblies.

Marler describes a method of tolerance analysis known as the Direct Linearization Method [13]. This method is based on linearizing the assembly equations using a first order Taylor's series expansion. For two-dimensional problems, each vector loop yields three constraint equations - closure in the x and y directions, and angular closure. Using

linear algebra to solve these equations leads to the matrix of tolerance sensitivities of the assembly to the corresponding independent variable. This matrix is used in forming root-sum-squares expressions which describe the statistical tolerances of the assembly. This process has been incorporated into the CATS tolerance analysis software which has evolved into commercial CAD applications.

With the DLM method it is not necessary to derive explicit expressions for the dependent variations in terms of independent variations. This method is also easily implemented in computer algorithms. One difficulty of this method when applied to a mechanism, is that the sensitivities have to be recalculated for every position of interest of the mechanism.

Fogarasy and Smith [7] use a similar method in analyzing the tolerances of a crank-slider, and circuit-breaker mechanism, with one difference. All of the angles used in their analysis are absolute, while the CATS method requires relative angles for the transmission of tolerance stack-up. This difference has prompted research into the necessity of absolute angles, which will be addressed later. Faik and Erdman applied this method of deriving sensitivities of a four-bar linkage [5]. These sensitivities were then used in a synthesis technique which optimized the performance of the four-bar mechanism.

Hanqi Huo described a graphical method of deriving the tolerance sensitivities using variation polygons [10]. Variation polygons are similar to velocity polygons used in traditional kinematics. Variations are represented as vectors in variation space.

Variation polygons have the advantage of being graphical in nature, and fairly intuitive.

This method is not easily automated however, because of its graphical nature.

An extension of the variation polygon method is using kinematic sensitivities extracted from kinematic software to find tolerance sensitivities. Lee and Gilmore use a method similar to the Direct Linearization Method to determine the kinematic sensitivities of mechanisms [12]. These sensitivities are then directly used to determine the statistical variation of the kinematic properties of mechanisms given link-length, pin-size, and pin clearance variations. No justification is given as to why the kinematic sensitivities are equivalent to the tolerance sensitivities. In addition, except for linkages, no explanation of the development of equivalent variational mechanisms is given.

Ogot and Gilmore [14], and Fenton, Cleghorn, and Fu suggest the use of kinematic sensitivities in an optimization routine which minimizes the output errors of mechanisms. Kinematic sensitivities found using computer-aided kinematic analysis are used to change the orientation of each part until optimum reliability of the assembly is reached. Tolerances are then adjusted according to the sensitivities, and the resulting distribution is found using a Monte Carlo simulation. Justification for the use of kinematic sensitivities is again neglected, as well the development of equivalent variational mechanisms.

All of the articles written outside BYU used absolute angles for both kinematic and tolerance analysis. Many researchers at BYU expressed the importance of relative angles [13,4,3], but didn't offer any justification. The 2-D joints and their associated degrees of freedom considered in tolerance analysis were formalized by Chun [4].

#### **1.4 Contributions of this Thesis**

This thesis provides the groundwork necessary for the use of kinematic sensitivities in tolerance analysis. It defines a library of equivalent variation mechanisms (EVMs) based on assembly joints for modeling dimensional variation. It also provides a systematic method for analyzing tolerances for the full range of motion of mechanisms as well as static assemblies, known as the Tolerance Analysis using Kinematic Sensitivities (TAKS) method.

## Chapter 2 Comparison of Kinematic and Tolerance Analyses

### 2.1 Kinematic Analysis of a Four Bar Mechanism

The four bar mechanism (Figure 2.1) is a common mechanism whose position and related equations are readily derived. It is ideal for demonstrating the relationship between kinematic and tolerance sensitivities and their application to engineering analysis. Kinematic analysis predicts the angular position, velocity and acceleration of Links 3 and 4 given the position, velocity and acceleration of Link 2. Tolerance analysis of the model predicts the position angular variation of Links 3 and 4 given the input position of Link 2, and the length variations of Links 1-4. Vector loop models are commonly used in both types of analysis. An appropriate vector loop for solving the kinematics of the four bar is shown in Figure 2.2.

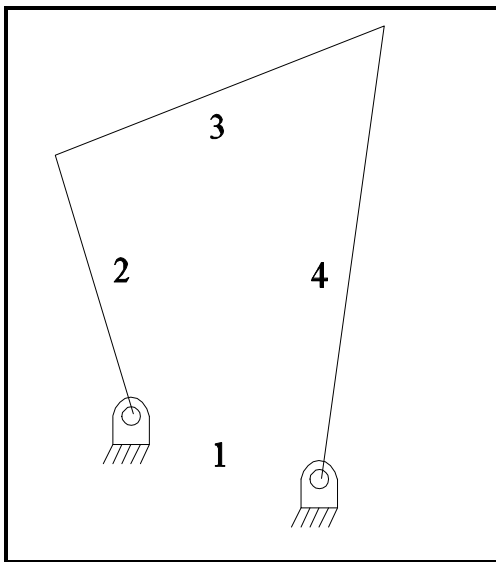


**Figure 2.1** A four bar mechanism.

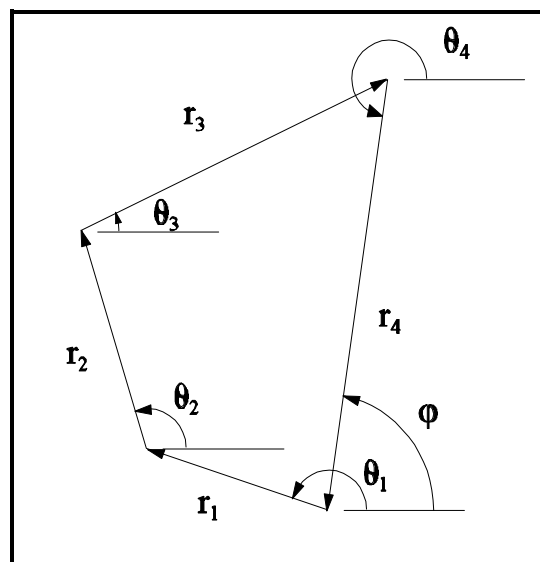


**Figure 2.2** The vector loop used in the kinematic analysis of the four bar.

The vector loop shown in Figure 2.2 yields the following closure equation:

$$r_1 e^{i(\mathbf{q}_1)} + r_2 e^{i(\mathbf{q}_2)} + r_3 e^{i(\mathbf{q}_3)} + r_4 e^{i(\mathbf{q}_4)} = 0 \quad (2.1)$$

This equation can be resolved into real and imaginary components, from which the angular position of Links 3 and 4 can be extracted for any successive position of Link 2.

The loop equations are then differentiated with respect to time yielding the following two equations:

$$\begin{aligned} \mathbf{w}_2 r_2 \sin \mathbf{q}_2 + \mathbf{w}_3 r_3 \sin \mathbf{q}_3 + \mathbf{w}_4 r_4 \sin \mathbf{q}_4 &= 0 \\ \mathbf{w}_2 r_2 \cos \mathbf{q}_2 + \mathbf{w}_3 r_3 \cos \mathbf{q}_3 + \mathbf{w}_4 r_4 \cos \mathbf{q}_4 &= 0 \end{aligned} \quad (2.2)$$

in matrix form:

$$[A]\mathbf{w}_2 + [B]\begin{Bmatrix} \mathbf{w}_3 \\ \mathbf{w}_4 \end{Bmatrix} = 0 \quad \text{where } [A] = \begin{bmatrix} r_2 \sin \mathbf{q}_2 \\ r_2 \cos \mathbf{q}_2 \end{bmatrix}, \text{ and } [B] = \begin{bmatrix} r_3 \sin \mathbf{q}_3 & r_4 \sin \mathbf{q}_4 \\ r_3 \cos \mathbf{q}_3 & r_4 \cos \mathbf{q}_4 \end{bmatrix} \quad (2.3)$$

Solving for the dependent variables  $\mathbf{w}_3$ , and  $\mathbf{w}_4$  and simplifying:

$$\begin{Bmatrix} \mathbf{w}_3 \\ \mathbf{w}_4 \end{Bmatrix} = [-B^{-1}A] \cdot \mathbf{w}_2 = \begin{bmatrix} \frac{r_2 (\cos \mathbf{q}_2 \sin \mathbf{q}_4 - \cos \mathbf{q}_4 \sin \mathbf{q}_2)}{r_3 (\cos \mathbf{q}_4 \sin \mathbf{q}_3 - \cos \mathbf{q}_3 \sin \mathbf{q}_4)} \\ \frac{r_2 (\cos \mathbf{q}_2 \sin \mathbf{q}_3 + \cos \mathbf{q}_3 \sin \mathbf{q}_2)}{r_4 (\cos \mathbf{q}_4 \sin \mathbf{q}_3 - \cos \mathbf{q}_3 \sin \mathbf{q}_4)} \end{bmatrix} \cdot \mathbf{w}_2 \quad (2.4)$$

For the four bar mechanism with fixed link lengths and position shown in Table 1:

$$\begin{Bmatrix} \mathbf{w}_3 \\ \mathbf{w}_4 \end{Bmatrix} = \begin{bmatrix} .2196 \\ .5966 \end{bmatrix} \cdot \mathbf{w}_2 \quad (2.5)$$

**Table 2.1** Link lengths and angular position data for numerical examples.

	Length	Absolute Angle	Relative Angle	Angular Velocity	Length Variation	Angular Variation	Angular Variation
Link	$r_i$	$2_i$	$''_i$	$T_i$	$dr_i$	$d2_i$	$d''_i$
1	25	180	0	0	1	0	0
2	18	90	270	1	1	1	1
3	44	25.95	295.95	<i>unknown</i>	1	<i>unknown</i>	<i>unknown</i>
4	40	248.65	222.70	<i>unknown</i>	1	<i>unknown</i>	<i>unknown</i>

The  $[-B^{-1}A]$  matrix (Equations 2.4, 2.6) is known as the Jacobian matrix. The rows of the Jacobian describe the ratio, or effect of  $w_2$  on  $w_3$ , and  $w_4$ . Thus, the Jacobian describes the kinematic sensitivity of the input  $\omega_2$  on the resulting angular velocities  $w_3$ , and  $w_4$ . Numerically, this means that the magnitude of  $\omega_3$  is 0.2196 of  $w_2$ , and  $w_4$  is 0.5967 of  $w_2$ . Traditional analyses relate the angular velocity of  $N$  (the angle of link four with respect to ground) to  $w_2$ . The angular velocity of  $N$  can be found by differentiating the geometric relationship  $N = q_4 - p$  yielding:  $\dot{f} = w_4$ .

## 2.2 Tolerance Analysis Using a Vector Loop

In tolerance analysis, small changes in link lengths caused by manufacturing variations result in variations from the nominal orientation of the links. Such variations accumulate, or stack up, in an assembly resulting in poor performance or badly fitting parts. Statistical tolerance analysis can be performed to predict the expected assembly variation when distributions of part variations are known. To allow for tolerance stack up to be transmitted through the vector chain, the angular position of each vector is defined relative to the preceding vector by means of the relative angles  $\acute{a}_i$ , as shown in Figure 2.3.

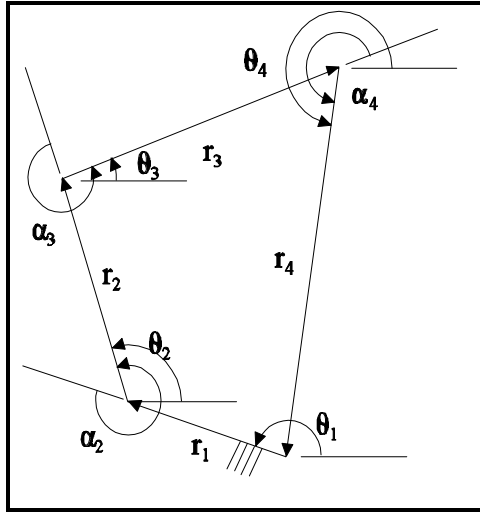


**Figure 2.3** A vector loop with relative angles used in the tolerance analysis of a four bar.

This vector loop yields the following vector equation:

$$r_1 e^{i(\mathbf{q}_1)} + r_2 e^{i(\mathbf{q}_1 + \mathbf{a}_2)} + r_3 e^{i(\mathbf{q}_1 + \mathbf{a}_2 + \mathbf{a}_3)} + r_4 e^{i(\mathbf{q}_1 + \mathbf{a}_2 + \mathbf{a}_3 + \mathbf{a}_4)} = 0 \quad (2.6)$$

where  $\mathbf{a}_2$ ,  $\mathbf{a}_3$ , and  $\mathbf{a}_4$  are the relative angles between adjacent links. Comparing to

Equation 2.6 to Equation 2.1 reveals the following relationships:

$$\mathbf{q}_2 = \mathbf{q}_1 + \mathbf{a}_2 \quad \mathbf{q}_3 = \mathbf{q}_2 + \mathbf{a}_3 \quad \mathbf{q}_4 = \mathbf{q}_3 + \mathbf{a}_4 \quad (2.7)$$

Substituting this into Equation 2.6, yields vector Equation 2.1:

$$r_1 e^{i(\mathbf{q}_1)} + r_2 e^{i(\mathbf{q}_2)} + r_3 e^{i(\mathbf{q}_3)} + r_4 e^{i(\mathbf{q}_4)} = 0$$

By taking the differential of the vector position Equation 2.6, we get:

$$\begin{aligned} & \cos \mathbf{q}_1 dr_1 + \cos \mathbf{q}_2 dr_2 + \cos \mathbf{q}_3 dr_3 + \cos \mathbf{q}_4 dr_4 - (r_2 \sin \mathbf{q}_2 + r_3 \sin \mathbf{q}_3 + r_4 \sin \mathbf{q}_4) d\mathbf{a}_2 \\ & - (r_3 \sin \mathbf{q}_3 + r_4 \sin \mathbf{q}_4) d\mathbf{a}_3 - r_4 \sin \mathbf{q}_4 d\mathbf{a}_4 = 0 \\ \\ & \sin \mathbf{q}_1 dr_1 + \sin \mathbf{q}_2 dr_2 + \sin \mathbf{q}_3 dr_3 + \sin \mathbf{q}_4 dr_4 + (r_2 \cos \mathbf{q}_2 + r_3 \cos \mathbf{q}_3 + r_4 \cos \mathbf{q}_4) d\mathbf{a}_2 \\ & + (r_3 \cos \mathbf{q}_3 + r_4 \cos \mathbf{q}_4) d\mathbf{a}_3 + r_4 \cos \mathbf{q}_4 d\mathbf{a}_4 = 0 \end{aligned} \quad (2.8)$$

where  $dr_i$  and  $d\acute{a}_i$  represent small changes in the lengths and angles, respectively.

Writing Equation 8 in matrix form:

$$[A] \begin{Bmatrix} d\mathbf{a}_2 \\ dr_1 \\ dr_2 \\ dr_3 \\ dr_4 \end{Bmatrix} + [B] \begin{Bmatrix} d\mathbf{a}_3 \\ d\mathbf{a}_4 \end{Bmatrix} = 0 \quad (2.9)$$

where  $[A] = \begin{bmatrix} (-r_2 \sin \mathbf{q}_2 - r_3 \sin \mathbf{q}_3 - r_4 \sin \mathbf{q}_4) & \cos \mathbf{q}_1 & \cos \mathbf{q}_2 & \cos \mathbf{q}_3 & \cos \mathbf{q}_4 \\ (r_2 \cos \mathbf{q}_2 + r_3 \cos \mathbf{q}_3 + r_4 \cos \mathbf{q}_4) & \sin \mathbf{q}_1 & \sin \mathbf{q}_2 & \sin \mathbf{q}_3 & \sin \mathbf{q}_4 \end{bmatrix}$

and  $[B] = \begin{bmatrix} (-r_3 \sin \mathbf{q}_3 - r_4 \sin \mathbf{q}_4) & -r_4 \sin \mathbf{q}_4 \\ (r_3 \cos \mathbf{q}_3 + r_4 \cos \mathbf{q}_4) & r_4 \cos \mathbf{q}_4 \end{bmatrix}$

Solving for the dependent variables ( $\alpha_3$ ,  $\alpha_4$ ) and writing the system in matrix form yields:

$$\begin{Bmatrix} d\mathbf{a}_3 \\ d\mathbf{a}_4 \end{Bmatrix} = [-B^{-1}A] \begin{Bmatrix} d\mathbf{a}_2 \\ dr_1 \\ dr_2 \\ dr_3 \\ dr_4 \end{Bmatrix} = [S_{i,j}] \begin{Bmatrix} d\mathbf{a}_2 \\ dr_1 \\ dr_2 \\ dr_3 \\ dr_4 \end{Bmatrix} \quad (2.10)$$

$[A]$  and  $[B]$  are the coefficient matrices of the independent and dependent variables, respectively, which combine to form the tolerance sensitivity matrix  $[S]$ . This matrix defines the variation  $d\acute{a}_3$  and  $d\acute{a}_4$  as the sum of fractions of the variations  $d\acute{a}_2$ ,  $dr_1$ ,  $dr_2$ ,  $dr_3$ , and  $dr_4$ . For the four bar mechanism described in Table 1:

$$[A] = \begin{bmatrix} 0 & -1 & 0 & 0.8992 & -0.3641 \\ 25 & 0 & 1 & 0.4376 & -0.9314 \end{bmatrix} \quad [B] = \begin{bmatrix} 18 & 37.2546 \\ 25 & -14.5634 \end{bmatrix}$$

And,

$$\begin{Bmatrix} d\mathbf{a}_3 \\ d\mathbf{a}_4 \end{Bmatrix} = \begin{bmatrix} -0.7804 & 0.0122 & -0.0312 & -0.0246 & 0.0335 \\ 0.3770 & 0.0209 & 0.0151 & -0.0122 & -0.0064 \end{bmatrix} \begin{Bmatrix} d\mathbf{a}_2 \\ dr_1 \\ dr_2 \\ dr_3 \\ dr_4 \end{Bmatrix} = \begin{Bmatrix} -0.0136 \\ 0.0066 \end{Bmatrix} \quad (2.11)$$

This represents a single case tolerance analysis, (the predicted variations in an assembly due to the errors in one set of components). To predict the tolerance stack up statistically in a group of assemblies, the sensitivities may be used to form a root-sum-

squares expression  $d\mathbf{a}_i = \sqrt{\sum (S_{i,j} du_j)^2}$ , where  $du_1$  is the probable error in the input

position  $d\mathbf{a}_2$ , and  $du_{2,5}$  are the 36 tolerances of the manufacturing process used to produce the part lengths. This comes from statistical error analysis where probability distributions are added by adding variances, which are the standard deviations squared. For the four bar described in Table1:

$$d\mathbf{a}_3 = \sqrt{(-0.7804d\mathbf{a}_2)^2 + (0.0122dr_1)^2 + (-0.0312dr_2)^2 + (-0.0246dr_3)^2 + (0.0335dr_4)^2}$$

$$d\mathbf{a}_4 = \sqrt{(0.3770d\mathbf{a}_2)^2 + (0.0209dr_1)^2 + (0.0151dr_2)^2 + (-0.0122dr_3)^2 + (-0.0064dr_4)^2}$$

(2.12)

### 2.3 Relationship Between Kinematic and Tolerance Analysis

Comparison of the two analyses methods reveals many similarities. Both are based on the same vector loop which describes the mechanism. Kinematics determines the instantaneous velocities at a specified position of  $\theta_2$ . The kinematic analysis must be repeated for each position of the mechanism. Tolerance analysis determines the probable variation in angles at a specified position of  $\theta_2$ . Rather than a single assembly, it describes the probable variation from one assembly to the next. It is independent of time variation, but dependent on angular position and must be repeated for each position of  $\theta_2$ . Differences between the two models used in the analysis include the way that the angles are defined (absolute angles for kinematics, relative angles for tolerance analysis), the input variables considered (link position and velocity for kinematics, angle and link length variations for tolerance analysis), and the output variables (link position and velocity for kinematics, angle and link length variations for tolerance analysis).

**Table 2.2** A comparison of kinematic and tolerance analysis.

	<b>Kinematic Analysis</b>	<b>Tolerance Analysis</b>
Describes:	Instantaneous velocities.	Probable assembly variations
Input:	Link positions and input link velocity	Independent variations in angles and link lengths
Output:	Output link velocities	Dependent variations in angles and link lengths
Angles:	Absolute	Relative

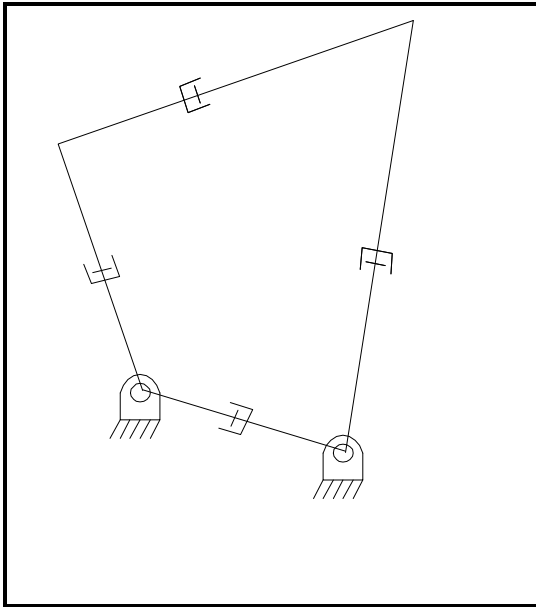


**Figure 2.4** A four bar mechanism with 'growing links'.

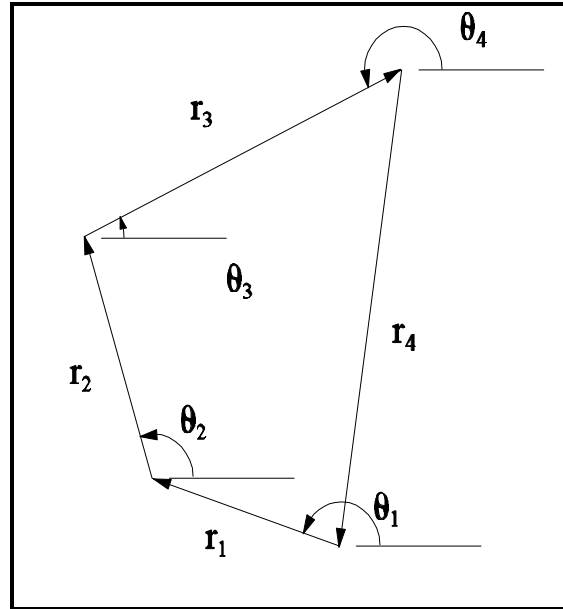


**Figure 2.5** The vector loop used in the kinematic analysis of the four bar.

The similarities indicate that it may be possible to perform a tolerance analysis on a mechanism using results from the kinematic analysis. The differences between the analyses suggest changes in the kinematic model which would allow both kinematic and tolerance analysis. A modified kinematic model is shown in Figure 2.4. Inclusion of slider joints in each of the links of the kinematic model allows the links to 'grow' at a specified rate, simulating link length variation used in the tolerance analysis. The angles remain defined as absolute, since that is how they are defined in most kinematic models.

#### 2.4 Kinematic Analysis of a Four-Bar with 'Growing Links'

For a kinematic analysis of the mechanism in Figure 4, we start again with the following vector Equation 2.1, repeated below:

$$r_1 e^{i(q_1)} + r_2 e^{i(q_2)} + r_3 e^{i(q_3)} + r_4 e^{i(q_4)} = 0$$

which when differentiated yields the following two equations:

$$\begin{aligned} \dot{r}_1 \cos \mathbf{q}_1 + \dot{r}_2 \cos \mathbf{q}_2 + \dot{r}_3 \cos \mathbf{q}_3 + \dot{r}_4 \cos \mathbf{q}_4 - \mathbf{w}_2 r_2 \sin \mathbf{q}_2 - \mathbf{w}_3 r_3 \sin \mathbf{q}_3 - \mathbf{w}_4 r_4 \sin \mathbf{q}_4 &= 0 \\ \dot{r}_1 \sin \mathbf{q}_1 + \dot{r}_2 \sin \mathbf{q}_2 + \dot{r}_3 \sin \mathbf{q}_3 + \dot{r}_4 \sin \mathbf{q}_4 + \mathbf{w}_2 r_2 \cos \mathbf{q}_2 + \mathbf{w}_3 r_3 \cos \mathbf{q}_3 + \mathbf{w}_4 r_4 \cos \mathbf{q}_4 &= 0 \end{aligned} \quad (2.13)$$

Where the  $\dot{r}_i$  are the relative sliding velocities in each slider joint. In matrix form,

$$[A] \begin{Bmatrix} \mathbf{w}_2 \\ \dot{r}_1 \\ \dot{r}_2 \\ \dot{r}_3 \\ \dot{r}_4 \end{Bmatrix} + [B] \begin{Bmatrix} \mathbf{w}_3 \\ \mathbf{w}_4 \end{Bmatrix} = 0 \quad (2.14)$$

where  $A = \begin{bmatrix} -r_2 \sin \mathbf{q}_2 & \cos \mathbf{q}_1 & \cos \mathbf{q}_2 & \cos \mathbf{q}_3 & \cos \mathbf{q}_4 \\ r_2 \cos \mathbf{q}_2 & \sin \mathbf{q}_1 & \sin \mathbf{q}_2 & \sin \mathbf{q}_3 & \sin \mathbf{q}_4 \end{bmatrix}$  and  $B = \begin{bmatrix} -r_3 \sin \mathbf{q}_3 & -r_4 \sin \mathbf{q}_4 \\ r_3 \cos \mathbf{q}_3 & r_4 \cos \mathbf{q}_4 \end{bmatrix}$

Solving for the dependent variables  $\mathbf{w}_3$ , and  $\mathbf{w}_4$ :

$$\begin{Bmatrix} \mathbf{w}_3 \\ \mathbf{w}_4 \end{Bmatrix} = [-B^{-1}A] \begin{Bmatrix} \mathbf{w}_2 \\ \dot{r}_1 \\ \dot{r}_2 \\ \dot{r}_3 \\ \dot{r}_4 \end{Bmatrix} = [J_{i,j}] \begin{Bmatrix} \mathbf{w}_2 \\ \dot{r}_1 \\ \dot{r}_2 \\ \dot{r}_3 \\ \dot{r}_4 \end{Bmatrix} \quad (2.15)$$

Again,  $[A]$  and  $[B]$  are the coefficient matrices of the dependent and independent variables, respectively, which when multiplied form the kinematic sensitivity matrix  $[J]$ .

The elements of  $[J]$  are functions of link angles, so  $[J]$  must be re-evaluated at each

position of input crank  $r_2$ . Setting the slider velocities  $\dot{r}_1 = \dot{r}_2 = \dot{r}_3 = \dot{r}_4 = 0$  yields the

traditional kinematic solution for constant link lengths.

For the variable link lengths and angular positions specified in Table 1:

$$\begin{Bmatrix} \mathbf{w}_3 \\ \mathbf{w}_4 \end{Bmatrix} = \begin{bmatrix} 0.2196 & 0.0122 & -0.0312 & -0.0246 & 0.0335 \\ 0.5966 & 0.0331 & -0.0161 & -0.0369 & 0.0271 \end{bmatrix} \begin{Bmatrix} \mathbf{w}_2 \\ \dot{r}_1 \\ \dot{r}_2 \\ \dot{r}_3 \\ \dot{r}_4 \end{Bmatrix} = \begin{Bmatrix} 0.0038 \\ 0.0104 \end{Bmatrix} \quad (2.16)$$

Recalling the tolerance analysis results:

$$\begin{Bmatrix} d\mathbf{a}_3 \\ d\mathbf{a}_4 \end{Bmatrix} = \begin{bmatrix} -0.7804 & 0.0122 & -0.0312 & -0.0246 & 0.0335 \\ 0.3770 & 0.0209 & 0.0151 & -0.0122 & -0.0064 \end{bmatrix} \begin{Bmatrix} d\mathbf{a}_2 \\ dr_1 \\ dr_2 \\ dr_3 \\ dr_4 \end{Bmatrix} = \begin{Bmatrix} -0.0136 \\ 0.0066 \end{Bmatrix}$$

A comparison of the two analyses shows that the Jacobian matrices have several identical terms. A closer look reveals that the terms in the  $\dot{\mathbf{u}}_4$  equation are the difference of the  $d\dot{\mathbf{a}}_3$  and  $d\dot{\mathbf{a}}_4$  equations from Equation 2.11. This is due to the relationship between the absolute and relative angles, which will be discussed in greater detail later.

## 2.5 Using Kinematic Sensitivities in Tolerance Analysis

The kinematic sensitivity matrix relates  $\mathbf{w}_3$  and  $\mathbf{w}_4$  to  $\mathbf{w}_2$ ,  $\dot{r}_1$ ,  $\dot{r}_2$ ,  $\dot{r}_3$  and  $\dot{r}_4$ . The tolerance sensitivity matrix relates  $d\dot{\mathbf{a}}_3$  and  $d\dot{\mathbf{a}}_4$  to  $d\dot{\mathbf{a}}_2$ ,  $dr_1$ ,  $dr_2$ ,  $dr_3$ , and  $dr_4$ . These relationships are represented by matrix Equations 2.10 and 2.15, which can also be written:

$$\begin{aligned} \mathbf{w}_3 &= J_{1,1}\mathbf{w}_2 + J_{1,2}\dot{r}_1 + J_{1,3}\dot{r}_2 + J_{1,4}\dot{r}_3 + J_{1,5}\dot{r}_4 \\ \mathbf{w}_4 &= J_{2,1}\mathbf{w}_2 + J_{2,2}\dot{r}_1 + J_{2,3}\dot{r}_2 + J_{2,4}\dot{r}_3 + J_{2,5}\dot{r}_4 \end{aligned} \quad \text{and} \quad (2.17)$$

$$\begin{aligned}
d\mathbf{a}_3 &= S_{1,1}d\mathbf{a}_2 + S_{1,2}dr_1 + S_{1,3}dr_2 + S_{1,4}dr_3 + S_{1,5}dr_4 \\
d\mathbf{a}_4 &= S_{2,1}d\mathbf{a}_2 + S_{2,2}dr_1 + S_{2,3}dr_2 + S_{2,4}dr_3 + S_{2,5}dr_4
\end{aligned} \tag{2.18}$$

Equations 2.17 and 2.18 are very similar. Both describe variations of the output angles 3 and 4. The equations differ in how the angles are defined, and the type of variation that is described. These differences are resolved using the relationship between the relative and absolute angles found Equation 2.7:

$$\mathbf{a}_3 = \mathbf{q}_3 - \mathbf{q}_2 \quad \mathbf{a}_4 = \mathbf{q}_4 - \mathbf{q}_3$$

the differential of which is:

$$\begin{aligned}
d\mathbf{a}_3 &= d\mathbf{q}_3 - d\mathbf{q}_2 & d\mathbf{a}_4 &= d\mathbf{q}_4 - d\mathbf{q}_3 \\
d\mathbf{q}_3 &= d\mathbf{a}_3 + d\mathbf{q}_2 & d\mathbf{q}_4 &= d\mathbf{a}_4 + d\mathbf{q}_3
\end{aligned} \tag{2.19}$$

Equation 2.19 describes the absolute angular variation  $d\mathbf{e}_i$  in terms of relative angular variation,  $d\mathbf{a}_i$ . Considering these variations as occurring over small increments of time (dividing Equation 2.19 by  $dt$ ) allows us to view small changes in angles as pseudo-velocities, as shown in Equation 2.20.

$$\begin{aligned}
\frac{d\mathbf{q}_3}{dt} &= \frac{d\mathbf{q}_2}{dt} + \frac{d\mathbf{a}_3}{dt} & \frac{d\mathbf{q}_4}{dt} &= \frac{d\mathbf{q}_3}{dt} + \frac{d\mathbf{a}_4}{dt}
\end{aligned} \tag{2.20}$$

Rewriting Equation 2.17:

$$\begin{aligned}
\frac{d\mathbf{q}_3}{dt} &= J_{1,1} \frac{d\mathbf{q}_2}{dt} + J_{1,2} \frac{dr_1}{dt} + J_{1,3} \frac{dr_2}{dt} + J_{1,4} \frac{dr_3}{dt} + J_{1,5} \frac{dr_4}{dt} \\
\frac{d\mathbf{q}_4}{dt} &= J_{2,1} \frac{d\mathbf{q}_2}{dt} + J_{2,2} \frac{dr_1}{dt} + J_{2,3} \frac{dr_2}{dt} + J_{2,4} \frac{dr_3}{dt} + J_{2,5} \frac{dr_4}{dt}
\end{aligned}$$

Substituting the expression for  $d2_3/dt$ ,  $d2_4/dt$  into Equation 2.20 and solving for

$d\mathbf{a}_3/dt$ ,  $d\mathbf{a}_4/dt$  we get:

$$\begin{aligned} \frac{d\mathbf{a}_3}{dt} &= (J_{1,1} - 1) \frac{d\mathbf{q}_2}{dt} + J_{1,2} \frac{dr_1}{dt} + J_{1,3} \frac{dr_2}{dt} + J_{1,4} \frac{dr_3}{dt} + J_{1,5} \frac{dr_4}{dt} \\ \frac{d\mathbf{a}_4}{dt} &= (J_{2,1} - J_{1,1}) \frac{d\mathbf{q}_2}{dt} + (J_{2,2} - J_{1,2}) \frac{dr_1}{dt} + (J_{2,3} - J_{1,3}) \frac{dr_2}{dt} + (J_{2,4} - J_{1,4}) \frac{dr_3}{dt} + (J_{2,5} - J_{1,5}) \frac{dr_4}{dt} \end{aligned} \quad (2.21)$$

In matrix form:

$$\begin{Bmatrix} \frac{d\mathbf{a}_3}{dt} \\ \frac{d\mathbf{a}_4}{dt} \end{Bmatrix} = \begin{bmatrix} J_{1,1} - 1 & J_{1,2} & J_{1,3} & J_{1,4} & J_{1,5} \\ J_{2,1} - J_{1,1} & J_{2,2} - J_{1,2} & J_{2,3} - J_{1,3} & J_{2,4} - J_{1,4} & J_{2,5} - J_{1,5} \end{bmatrix} \begin{Bmatrix} \frac{d\mathbf{q}_2}{dt} \\ \frac{dr_1}{dt} \\ \frac{dr_2}{dt} \\ \frac{dr_3}{dt} \\ \frac{dr_4}{dt} \end{Bmatrix} \quad (2.22)$$

Multiplying the entire equation by  $dt$  (considering the variations once

again as independent from time) yields Equation 2.23:

$$\begin{Bmatrix} d\mathbf{a}_3 \\ d\mathbf{a}_4 \end{Bmatrix} = \begin{bmatrix} J_{1,1} - 1 & J_{1,2} & J_{1,3} & J_{1,4} & J_{1,5} \\ J_{2,1} - J_{1,1} & J_{2,2} - J_{1,2} & J_{2,3} - J_{1,3} & J_{2,4} - J_{1,4} & J_{2,5} - J_{1,5} \end{bmatrix} \begin{Bmatrix} d\mathbf{q}_2 \\ dr_1 \\ dr_2 \\ dr_3 \\ dr_4 \end{Bmatrix} = [J_m] \begin{Bmatrix} d\mathbf{q}_2 \\ dr_1 \\ dr_2 \\ dr_3 \\ dr_4 \end{Bmatrix} \quad (2.23)$$

Where  $[J_m]$  is the modified kinematic sensitivities matrix. Numerically,

$$\begin{Bmatrix} d\mathbf{a}_3 \\ d\mathbf{a}_4 \end{Bmatrix} = \begin{bmatrix} -0.7804 & 0.0122 & -0.0312 & -0.0246 & 0.0335 \\ 0.3770 & 0.0209 & 0.0151 & -0.0122 & -0.0064 \end{bmatrix} \begin{Bmatrix} d\mathbf{q}_2 \\ dr_1 \\ dr_2 \\ dr_3 \\ dr_4 \end{Bmatrix} = \begin{Bmatrix} -0.0136 \\ 0.0066 \end{Bmatrix} \quad (2.24)$$

Equation 2.24 is identical to the single case tolerance sensitivities previously found using the kinematic sensitivities. These sensitivities can be used to form a root-sum-square expression used in a statistical analysis of the mechanism as shown below.

$$\begin{aligned}
 d\mathbf{a}_3 &= \sqrt{(-0.7804d\mathbf{q}_2)^2 + (0.0122dr_1)^2 + (-0.0312dr_2)^2 + (-0.0246dr_3)^2 + (0.0335dr_4)^2} \\
 d\mathbf{a}_4 &= \sqrt{(0.3770\mathbf{q}_2)^2 + (0.0209dr_1)^2 + (0.0151dr_2)^2 + (-0.01223dr_3)^2 + (-0.0064dr_4)^2}
 \end{aligned}
 \tag{2.25}$$

The tolerance sensitivity matrix from Equation 2.24 can be obtained directly from the Jacobian matrix in Equation 2.16 using row operations performed on Equation 2.16 through the use of a transformation matrix  $[T]$ , as shown in Appendix A.

Note that a full tolerance analysis of the four-bar mechanism in Figure 2.1 would include the variation in the length and angle of the ground link,  $r_1$ . The variation in length of  $r_1$  has been considered through the inclusions of a slider element in the link. The angular variation of  $r_1$  may easily be included in the analysis by considering it as a known pseudo-velocity in the derivation of the kinematic equations. In this derivation the angular variation of  $r_1$  has been neglected allowing for a clearer demonstration of the relationship between kinematic and tolerance analyses.

## 2.6 Summary

It has been shown that tolerance analysis of a mechanism can be performed using the kinematic sensitivities of the mechanism when appropriate kinematic elements are included (slider joints in each link in our example). This is possible because of the relationship between kinematic and tolerance analysis. This relationship exists because

both analyses are based on the same vector loop. Three major differences in the analyses exist: how the angles are defined, variable vs. fixed link lengths, and how the derivatives of the vector loop equations are interpreted. These differences are resolved using the relationships between absolute and relative angles, derived from a comparison of the two loop equations. The differential of the loop relationships can be interpreted as pseudo-velocities, which, through substitution, can be used to derive tolerance sensitivities. A root-sum square expression can then be formed which includes the effects of tolerance stack-up.

Subsequent chapters will describe a systematic approach for applying this method, in addition to a demonstration of this method using the kinematic analysis software ADAMS.

The four-bar mechanism was easily modified to account for length variations because it only consisted of straight pin jointed links. We will see in the next chapters, that other types of dimensional variations will require more complex modifications in order to represent them in a kinematic model.

## Chapter 3 Kinematic Analysis of Static Assemblies

### 3.1 The One-Way Clutch

The one-way clutch, as described by Fortini [8], is shown in Figure 3.1. Clockwise rotation of the ring causes the roller to wedge between the ring and the hub, forcing the hub to rotate with the ring. The rollers disengage as the ring rotates counter-clockwise, allowing the hub to remain stationary as the ring rotates. In the past, this type of clutch was commonly used in lawn mower pull starter assemblies.

The pressure angle,  $M$ , has to be between 5 and 9 degrees for the clutch to operate properly. Angles larger than this prevent the clutch from engaging. Smaller angles prevent the clutch from disengaging. The ideal pressure angle is 7 degrees. Internal adjustments of length  $b$  and angle  $M$  are required to accommodate dimensional variations in the hub half width,  $a$ , the roller radius,  $c$ , and the ring radius,  $f$ . These internal adjustments are also known as kinematic variations, which can be represented nicely in a kinematic model of the static assembly.

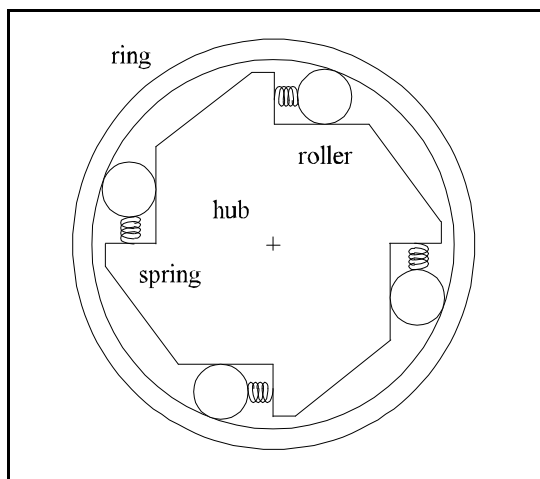


**Figure 3.1** One way clutch assembly.

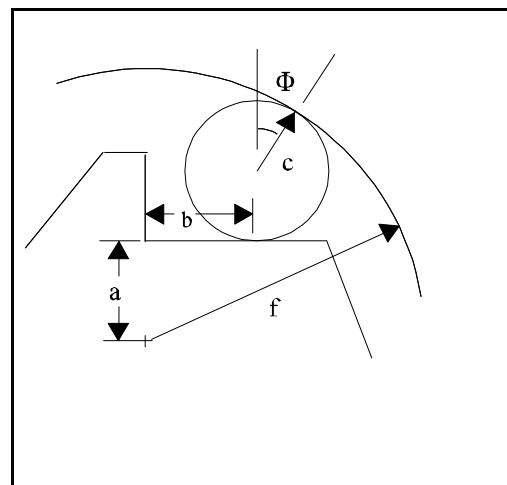


**Figure 3.2** Relevant dimensions for the clutch.

Tolerance analysis only considers the engaged position of the clutch. Other positions of the clutch are not critical, allowing us to view the clutch as a static assembly. This chapter demonstrates the application of the TAKS method to static assemblies. A tolerance analysis of the one-way clutch using traditional techniques will be presented first. An equivalent variational mechanism for the clutch will then be developed, and used to derive kinematic sensitivities. A final tolerance analysis, using the kinematic sensitivities, will then be presented. Dimensions and tolerances for the clutch are found in Table 3.1

**Table 3.1** Nominal dimensions and tolerances for the one-way clutch.

Dimension	Nominal Size	Initial Tolerance ( $\pm$ )	Kinematic Velocity
$\frac{1}{2}$ hub radius, $a$	27.645 mm	.050 mm	.050 mm/s
roller radius, $c$	11.430 mm	.010 mm	.010 mm/s
$\frac{1}{2}$ ring radius, $f$	50.800 mm	.0125 mm	.0125 mm/s
roller contact, $c$	4.8105 mm	<i>unknown</i>	<i>unknown</i>
pressure angle, $M$	$7.0184^{\text{N}}$	<i>unknown</i>	<i>unknown</i>

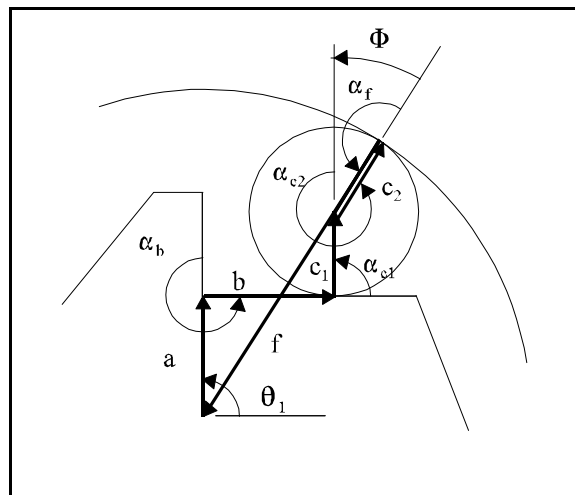


**Figure 3.3** The vector loop used to solve the clutch tolerance problem.

### 3.2 Tolerance Analysis of a One-Way Clutch Using a Vector Loop Approach

The vector loop from Figure 3 yields the following vector equation:

$$ae^{iq_1} + be^{i(q_1+a_b)} + c_1e^{i(q_1+a_b+a_{c1})} + c_2e^{i(q_1+a_b+a_{c1}+a_{c2})} + fe^{i(q_1+a_b+a_{c1}+a_{c2}+a_f)} = 0 \quad (3.1)$$

The differential of this vector loop is:

$$da \cdot e^{iq_1} + db \cdot e^{i(q_1+a_b)} + dc \cdot (e^{i(q_1+a_b+a_{c1})} + e^{i(q_1+a_b+a_{c1}+a_{c2})}) + da_{c2} (cie^{i(q_1+a_b+a_{c1}+a_{c2})} + fie^{i(q_1+a_b+a_{c1}+a_{c2}+a_f)}) + df \cdot e^{i(q_1+a_b+a_{c1}+a_{c2}+a_f)} = 0 \quad (3.2)$$

Where  $dc_1 = dc_2 = dc$ , since  $c_1$  and  $c_2$  are the same dimension. Note that the differential is a function of  $d''_{c2}$ . Original angular specifications were placed on the angle  $M$ . Since  $M = 360 - ''_{c2}$ ,  $dM = -d''_{c2}$ . By substitution:

$$da \cdot e^{iq_a} + db \cdot e^{i(q_a+a_b)} + dc \cdot (e^{i(q_a+a_b+a_{c1})} + e^{i(q_a+a_b+a_{c1}+a_{c2})}) - df \cdot (cie^{i(q_a+a_b+a_{c1}+a_{c2})} + fie^{i(q_a+a_b+a_{c1}+a_{c2}+a_f)}) + df \cdot e^{i(q_a+a_b+a_{c1}+a_{c2}+a_f)} = 0 \quad (3.3)$$

Tolerance analysis traditionally uses relative angles to describe angular positions.

This is useful since tolerance specifications are often given in relative coordinates. The vector loop with each vector described using absolute angles given in Equation 4.

$$ae^{iq_1} + be^{iq_b} + c_1e^{iq_{c1}} + c_2e^{iq_{c2}} + fe^{iq_f} = 0 \quad (3.4)$$

Comparing Equations 1 and 3 shows the following equalities:

$$\begin{aligned} \mathbf{q}_b &= \mathbf{q}_1 + \mathbf{a}_b & \mathbf{q}_{c2} &= \mathbf{q}_1 + \mathbf{a}_b + \mathbf{a}_{c1} + \mathbf{a}_{c2} \\ \mathbf{q}_c &= \mathbf{q}_1 + \mathbf{a}_b + \mathbf{a}_{c1} & \mathbf{q}_f &= \mathbf{q}_1 + \mathbf{a}_b + \mathbf{a}_{c1} + \mathbf{a}_{c2} + \mathbf{a}_f \end{aligned} \quad (3.5)$$

which allows us to simplify Equation 3.3:

$$\begin{aligned} da \cdot e^{iq_a} + db \cdot e^{iq_b} + dc(e^{iq_{c1}} + e^{iq_{c2}}) - d\mathbf{f}(c_1 e^{iq_{c1}} + f e^{if}) \\ + df \cdot e^{iq_f} = 0 \end{aligned} \quad (3.6)$$

Resolving this vector equation into its x and y components yields two scalar equations:

$$\begin{aligned} \cos \mathbf{q}_1 da + \cos(\mathbf{q}_b) db + (\cos \mathbf{q}_{c1} + \cos \mathbf{q}_{c2}) dc + \cos \mathbf{q}_f df \\ + (c \sin \mathbf{q}_{c2} + f \sin \mathbf{q}_f) d\mathbf{f} = 0 \\ \sin \mathbf{q}_1 da + \sin(\mathbf{q}_b) db + (\sin \mathbf{q}_{c1} + \sin \mathbf{q}_{c2}) dc + \sin \mathbf{q}_f df \\ - (c \cos \mathbf{q}_{c2} + f \cos \mathbf{q}_f) d\mathbf{f} = 0 \end{aligned} \quad (3.7)$$

Writing this in matrix notation:

$$\begin{bmatrix} \cos \mathbf{q}_1 & (\cos \mathbf{q}_{c1} + \cos \mathbf{q}_{c2}) & \cos \mathbf{q}_f \\ \sin \mathbf{q}_1 & (\sin \mathbf{q}_{c1} + \sin \mathbf{q}_{c2}) & \sin \mathbf{q}_f \end{bmatrix} \begin{Bmatrix} da \\ dc \\ df \end{Bmatrix} + \begin{bmatrix} \cos \mathbf{q}_b & (c \sin \mathbf{q}_{c2} + f \sin \mathbf{q}_f) \\ \sin \mathbf{q}_b & (-c \cos \mathbf{q}_{c2} - f \cos \mathbf{q}_f) \end{bmatrix} \begin{Bmatrix} db \\ d\mathbf{f} \end{Bmatrix} = 0 \quad (3.8)$$

which is in the form

$$[A] \begin{Bmatrix} da \\ dc \\ df \end{Bmatrix} + [B] \begin{Bmatrix} db \\ d\mathbf{f} \end{Bmatrix} = 0 \quad (3.9)$$

Solving for the dependent variables  $db$  and  $dM$ :

$$\begin{Bmatrix} db \\ d\mathbf{f} \end{Bmatrix} = [-B^{-1}A] \begin{Bmatrix} da \\ dc \\ df \end{Bmatrix} = [S_{i,j}] \begin{Bmatrix} da \\ dc \\ df \end{Bmatrix} \quad (3.10)$$

For the clutch with dimensions found in Table 3.1:

$$\begin{Bmatrix} db \\ df \end{Bmatrix} = \begin{bmatrix} -8.1227 & -16.306 & 8.1841 \\ -0.2078 & -0.41420 & 0.2063 \end{bmatrix} \begin{Bmatrix} da \\ dc \\ df \end{Bmatrix} \quad (3.11)$$

Equation 3.10 can be used to find the variance of  $b$  and  $c_2$  given individual part variations of  $a$ ,  $c$ , and  $f$ . The tolerance sensitivities,  $S_{ij}$  can be used to develop worst case and statistical tolerance models.

### 3.4 Equivalent Variational Mechanisms

Additional kinematic elements representing dimensional variations must be added to the kinematic model, creating an equivalent variational mechanism (EVM). For the four-bar, slider joints in each link represent the dimensional variations of the links. Likewise, variations in the hub width, and ring and roller radii can also be represented with slider joints. All of the links representing the radius of the roller are required to ‘grow’ at the same rate. This is accomplished by applying the same velocity to each of the respective joints. An equivalent variational mechanism for the clutch is presented in Figure 3.4.

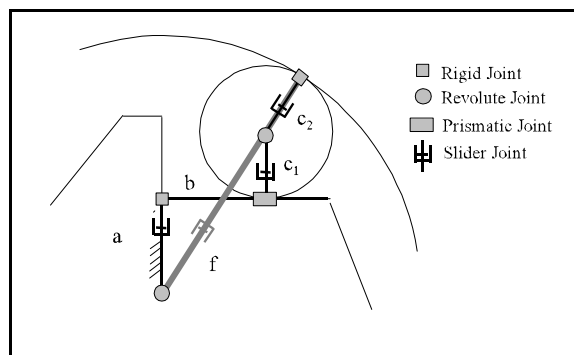


**Figure 3.4** A mechanism variationally equivalent to the one way clutch.

In addition to representing dimensional variations, EVMs must correctly represent assembly constraints. For instance, Links  $c_2$  and  $f$  must always be co-linear, assuming that both the roller and the ring are perfect circles. This assumption is valid as long as we are not considering form variations. A fixed joint is placed between these two links to keep them co-linear.

Additional joints representing the appropriate degrees of freedom are placed between links. Chapter 4 discusses the creation and use of EVMs in greater detail.

### 3.5 Kinematic Analysis of the Equivalent Variational Mechanism

The vector loop used in the kinematic analysis of the EVM is identical to the vector loop used in the tolerance analysis, shown in Figure 3.3, but the angles are the absolute angles, orienting each vector relative to the positive x-axis.

The vector loop in Figure 3.3 yields the following position equation:

$$ae^{iq_a} + be^{iq_b} + c_1e^{iq_{c1}} + c_2e^{iq_{c2}} + fe^{i(q_f)} = 0 \quad (3.12)$$

It should be noted that  $q_f$  is not independent. Rather, due to the fixed joint between  $c_2$  and  $f$ ,

$$q_f = q_{c2} + 180$$

The derivative of the position equation is the velocity equation:

$$\begin{aligned} \dot{a}e^{iq_a} + \dot{b}e^{iq_b} + \dot{c}_1(e^{iq_{c1}} + e^{iq_{c2}}) + \dot{q}_{c2}(c_1e^{iq_{c2}} + fe^{i(q_f)}) \\ + \dot{f}e^{i(q_f)} = 0 \end{aligned} \quad (3.13)$$

Equation 3.13 can be resolved into real and imaginary components:

$$\begin{aligned} \cos \mathbf{q}_1 \dot{a} + \cos \mathbf{q}_b \dot{b} + (\cos \mathbf{q}_{c1} + \cos \mathbf{q}_{c2}) \dot{c} \\ + (-c_1 \sin \mathbf{q}_{c1} - f \sin \mathbf{q}_f) \dot{\mathbf{q}}_{c2} + \cos \mathbf{q}_f \dot{f} = 0 \end{aligned} \quad (3.14)$$

$$\begin{aligned} \sin \mathbf{q}_1 \dot{a} + \sin \mathbf{q}_b \dot{b} + (\sin \mathbf{q}_{c1} + \sin \mathbf{q}_{c2}) \dot{c} \\ + (c \cos \mathbf{q}_{c1} + f \cos \mathbf{q}_f) \dot{\mathbf{q}}_{c2} + \sin \mathbf{q}_f \dot{f} = 0 \end{aligned}$$

Rearranging this into matrix form

$$\begin{bmatrix} \cos \mathbf{q}_1 & (\cos \mathbf{q}_{c1} + \cos \mathbf{q}_{c2}) & \cos \mathbf{q}_f \\ \sin \mathbf{q}_1 & (\sin \mathbf{q}_{c1} + \sin \mathbf{q}_{c2}) & \sin \mathbf{q}_f \end{bmatrix} \begin{Bmatrix} \dot{a} \\ \dot{c}_1 \\ \dot{f} \end{Bmatrix} + \begin{bmatrix} \cos \mathbf{q}_b & (-c_2 \sin \mathbf{q}_{c1} - f \sin \mathbf{q}_f) \\ \sin \mathbf{q}_b & (c_2 \cos \mathbf{q}_{c1} + f \cos \mathbf{q}_f) \end{bmatrix} \begin{Bmatrix} \dot{b} \\ \dot{\mathbf{q}}_{c2} \end{Bmatrix} = 0 \quad (3.15)$$

Which is in the form:

$$[A] \begin{Bmatrix} \dot{a} \\ \dot{c}_1 \\ \dot{f} \end{Bmatrix} + [B] \begin{Bmatrix} \dot{b} \\ \dot{\mathbf{q}}_{c2} \end{Bmatrix} = 0 \quad (3.16)$$

Solving for the dependent variables,

$$\begin{Bmatrix} \dot{b} \\ \dot{\mathbf{q}}_{c2} \end{Bmatrix} = [-B^{-1}A] \begin{Bmatrix} \dot{a} \\ \dot{c}_1 \\ \dot{f} \end{Bmatrix} = [J_{i,j}] \begin{Bmatrix} \dot{a} \\ \dot{c}_1 \\ \dot{f} \end{Bmatrix} \quad (3.17)$$

For the clutch with dimensions described in Table 1:

$$\begin{Bmatrix} \dot{b} \\ \dot{\mathbf{q}}_{c2} \end{Bmatrix} = \begin{bmatrix} -8.1227 & -16.306 & 8.1841 \\ 0.2078 & 0.4142 & -0.2063 \end{bmatrix} \begin{Bmatrix} \dot{a} \\ \dot{c}_1 \\ \dot{f} \end{Bmatrix} \quad (3.18)$$

### 3.5 Applying Kinematic Analysis to Tolerance Analysis

The kinematic sensitivity matrix relates dependent velocities  $\dot{b}$  and  $\dot{\mathbf{q}}_{c2}$  to independent velocities,  $\dot{a}$ ,  $\dot{c}$ , and  $\dot{f}$ , while the tolerance sensitivity matrix relates dependent variations  $db$  and  $dM$  to independent variations  $da$ ,  $dc$ , and  $df$ . These relationships are expressed by matrix Equations 3.18 and 3.11, and can be written as:

$$\begin{aligned}\frac{db}{dt} &= J_{1,1} \frac{da}{dt} + J_{1,1} \frac{dc}{dt} + J_{1,1} \frac{df}{dt} \\ \frac{d\mathbf{q}_{c2}}{dt} &= J_{2,1} \frac{da}{dt} + J_{2,1} \frac{dc}{dt} + J_{2,1} \frac{df}{dt}\end{aligned}\quad \text{Velocity Equation (3.19)}$$

and,

$$\begin{aligned}db &= S_{1,1}da + S_{1,2}dc_1 + S_{1,3}df \\ d\mathbf{f} &= S_{2,1}da + S_{2,2}dc_1 + S_{2,3}df\end{aligned}\quad \text{Variation Equation (3.20)}$$

Considering the variations from Equation 3.20 as occurring over small periods of time,  $dt$ , yields the psuedo-velocities:

$$\begin{aligned}\frac{db}{dt} &= S_{1,1} \frac{da}{dt} + S_{1,1} \frac{dc}{dt} + S_{1,1} \frac{df}{dt} \\ \frac{d\mathbf{f}}{dt} &= S_{2,1} \frac{da}{dt} + S_{2,1} \frac{dc}{dt} + S_{2,1} \frac{df}{dt}\end{aligned}\quad (3.21)$$

Considering the variations from Equation 3.20 as psuedo-velocities is necessary to allow us to substitute the tolerance variables as velocities into Equation 3.19 of the kinematic analysis. This substitution allows us to solve for the tolerance variations as functions of the kinematic sensitivities.

Equation 3.19 expresses the rate of change of  $b$  and  $M$  corresponding to any combination of rates of change of  $a$ ,  $b$ , and  $f$ . If we choose the velocities  $\dot{a}$ ,  $\dot{c}$ , and  $\dot{f}$  equal in magnitude to the dimensional variations  $da$ ,  $db$ , and  $df$ , the resulting  $\dot{b}$ , and  $\dot{f}$  will be equal in magnitude to the variations  $db$  and  $dM$ . To estimate tolerance sensitivities we will need to develop a root-sum-squares expression as demonstrated with the four-bar mechanism.

The two sets of equations are not exactly alike because the velocity equation uses angle  $2_{c2}$  and the variation equation uses  $M$ . This can be remedied by taking the differential of the angular relationship from Equation 3.5:

$$d\mathbf{q}_{c2} = -d\mathbf{f}$$

Considering these differentials as occurring over small periods of time,  $dt$ :

$$\frac{d\mathbf{q}_{c2}}{dt} = -\frac{d\mathbf{f}}{dt} \quad (3.22)$$

Substituting this into Equation 3.19 yields:

$$\begin{aligned} \frac{db}{dt} &= J_{1,1} \frac{da}{dt} + J_{1,1} \frac{dc}{dt} + J_{1,1} \frac{df}{dt} \\ \frac{d\mathbf{f}}{dt} &= -J_{2,1} \frac{da}{dt} - J_{2,1} \frac{dc}{dt} - J_{2,1} \frac{df}{dt} \end{aligned} \quad (3.23)$$

Multiplying the entire equation by  $dt$  (considering the variations once again as independent from time) yields Equation 3.24:

$$\begin{aligned} db &= J_{1,1} da + J_{1,1} dc_1 + J_{1,1} de \\ d\mathbf{f} &= -J_{2,1} da - J_{2,1} dc_1 - J_{2,1} de \end{aligned} \quad (3.24)$$

Equation 3.24 represents the tolerance sensitivities for  $db$  and  $dM$  found using the kinematic sensitivities  $J_{i,j}$ .

### 3.6 Discussion of Results

Note that the only difference between the two sensitivity matrices is the definition of angles. The relationship between the absolute and relative angles found in Equation 3.22 was used to transform the kinematic jacobian matrix into the tolerance sensitivity matrix. For the clutch this transformation was simple and straightforward. The transformation used in the four-bar example was also based on the relationship between the absolute and relative angles, and was only slightly more complicated.

The question arises, is the transformation necessary at all? Using absolute angles yields results that are correct, but correct with respect to ground. Dimensional tolerance specifications, however, are always defined with respect to local part datums in relative coordinates. This makes the transformation to relative coordinates necessary.

The ability to use kinematic sensitivities in the tolerance analysis of static assemblies has several advantages. This method provides a tolerance analysis tool for designers who have access to kinematic analysis software, but don't have access to tolerance analysis software. In addition, this method provides an alternative, and often more intuitive, method of visualizing dimensional variations and their effects.

This chapter focused on the application of the TAKS method to a static assembly, rather than a mechanism. Chapter 4 presents a comprehensive set of the development of EVMs using a static assembly as an example. Chapter 5 presents the systematic approach for the TAKS method and applies the method using kinematic software, ADAMS.

## Chapter 4 Equivalent Variational Mechanisms

Kinematic analysis determines output positions and velocities of mechanisms with fixed dimensions. Resulting sensitivities don't include the effects of dimensional variation. Additional kinematic elements can be placed in the kinematic model to include the effects of dimensional variations in the kinematic sensitivities. These sensitivities can then be used in tolerance analysis of assemblies. The development of correct equivalent variational mechanisms (EVMs) is key to successfully using kinematically derived sensitivities in a tolerance analysis.

EVMs are straightforward and easily derived for many assemblies, such as the four-bar mechanism. The EVM for the four-bar only required the addition of slider joints in each link. EVMs are primarily based on combinations of three kinematic elements: slider, fixed, and revolute joints. Slider joints represent length variations and revolute joints represent angular variations. Revolute joints can be a part of the original assembly, or introduced as an element in the EVM. Fixed joints are also used to represent locations in the assembly where there is no relative motion between parts.

Assembly constraints are represented by their equivalent kinematic joints. For instance, the fixed joint between equivalent links  $c_2$  and  $f$  on the one-way clutch imposes the assembly requirement that these two links remain co-linear (a requirement derived from the parallel cylinder joint between the two links). Replacing the paired cylinders with two binary links was necessary so that radii variation could be added to the EVM,

since there is no simple mechanical element which can represent a changing radius as a kinematic input. Clearly, it is often more difficult to visualize the representation of assembly constraints in EVMs.

Figure 4.1 compares the steps used in kinematic and tolerance analysis. Viewing the two types of analyses side by side demonstrates their similarities. Both utilize network graphs and skeleton diagrams to develop vector loops describing the geometry of the assembly. As demonstrated by the one-way clutch, the kinematic and tolerance vector loops for an assembly may be identical. However, additional elements must be added to create an EVM suitable for obtaining information from a kinematic analysis. EVMs can be derived by first developing tolerance analysis vector loops for the assembly, then using the vector loops as a starting point, adding joints and constraints in combinations designed to represent dimensional variation, finally arriving at an EVM for the assembly.

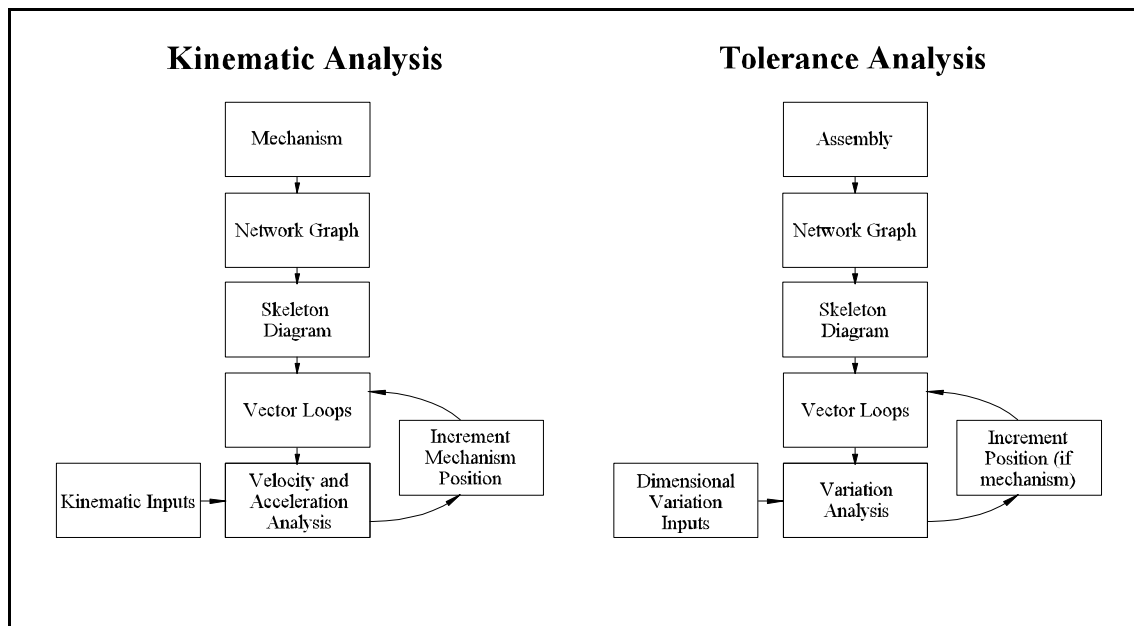


**Figure 4.1** Procedures for kinematic and tolerance analysis.

#### 4.1 Systematic Procedure for Creating Equivalent Variational Mechanisms (EVMs)

The following illustrates a step-by-step procedure for developing EVMs. Each step will be demonstrated on the stacked blocks problem (Figure 4.2). This assembly is especially instructive, as it includes four different assembly constraints.

The stacked blocks assembly consists of three parts: the frame, block, and cylinder. The gap between the high point of the cylinder and the frame adjusts to accommodate dimensional variations in the blocks. This gap is the critical dimension which we wish to control. The labeled dimensions locate features on each part which control the position and orientation of the mating parts and contribute to variation in the Gap. Tolerances, shown in the table, are specified according to process capabilities. We desire an estimate of the variation in the gap due to accumulated component variation.

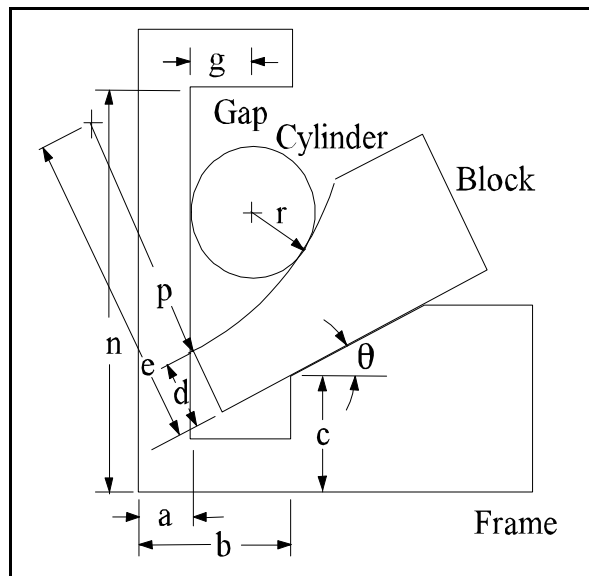


**Figure 4.2** The stacked blocks assembly and its dimensions.

Dim	Nominal	Tolerance
a	10.00 mm	$\pm .30$ mm
b	40.00 mm	$\pm .30$ mm
c	35.00 mm	$\pm .30$ mm
d	15.00 mm	$\pm 0$
e	55.00 mm	$\pm .30$ mm
n	75.00 mm	$\pm .50$ mm
g	10.00 mm	$\pm 0$
r	10.00 mm	$\pm .10$ mm
p	40.00 mm	$\pm .30$ mm
2	17.00°	$\pm 1^\circ$

Dimensions  $d$  and  $g$  are both shown on the drawing as un-toleranced reference dimensions. Neither  $d$  nor  $g$  is a contributing source of variation. The variation in  $d$  and  $g$  is determined by other dimensions. Dimension  $g$  locates the point of the frame directly above the highest point of the cylinder and varies with  $r$ . Dimension  $d$  is equal to the difference between dimensions  $e$  and  $p$ .

## 4.2 Developing a Vector loop

The first step in creating an EVM is to develop the vector loops describing the assembly. This requires building a network graph and skeleton diagram for the assembly, while placing vectors according to defined rules.

### 4.2.1 Network Graphs

Network graphs, also called assembly graphs, are helpful in determining the number of vector loops required to describe an assembly, as well as the paths that the vector loops should follow. The graphs are a simplified representation of the individual assembly components and joints between the components. A network graph for the stacked blocks is shown in Figure 4.3.

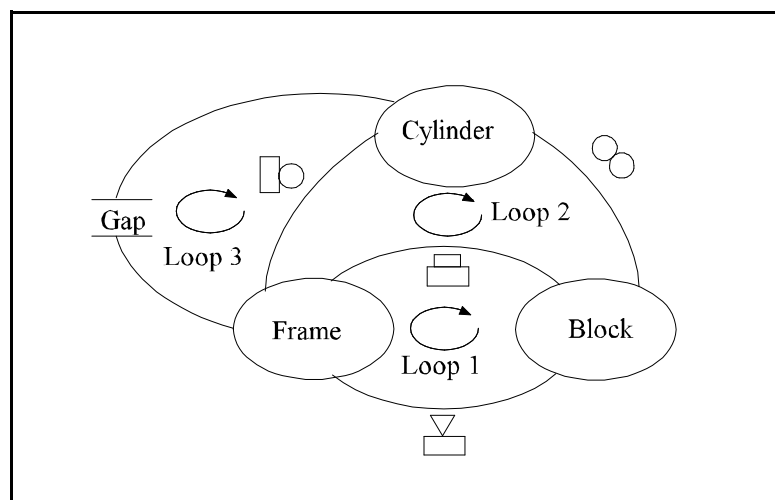


**Figure 4.3** A network graph for the stacked blocks problem.

Parts in the stacked block assembly are represented by ovals. Lines between the parts represent joints. Symbols have been added to these lines specifying the type of joints between mating parts. The number of closed loops required to describe the assembly are easily determined by inspection. Closed loops 1 and 2 on the graph represent assembly constraints. Open loop 3 describes the critical assembly gap. The network graph also shows the parts and joints that each vector loop must traverse. Rules describing the creation of vector loops are described in section 4.1.5. Several additional modeling elements (part and feature datum reference frames, and kinematic joints), must be located on the assembly before vectors can be defined.

#### **4.2.2 Feature and Part Datum Reference Frames**

Datum reference frames (DRF) are local coordinate systems used to define the part geometry. DRFs must be created for each part (Figure 4.4), and are preferably located at the datum planes used to define the part. All vector loops traversing a part must pass through the part DRF. Feature datums are reference axes used to locate and orient individual features on a part. Figure 4.4 illustrates the DRF located on each part. Notice that the Block DRF is rotated. Each datum axis is fixed to the part and oriented with it. The large radius feature on the Block is located by means of a cylindrical feature datum whose position is defined relative to the Block DRF.

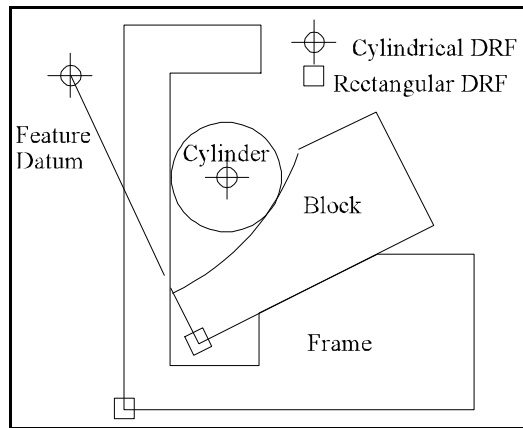


**Figure 4.4** Part and Feature Datum Reference Frames.

### 4.2.3 Kinematic Joints

Kinematic joints describe interactions between parts in the assembly. The joints describe how the parts move relative to each other in response to dimensional variation. Joint types commonly used in 2-D tolerance analysis and their associated degrees of freedom are shown in Figure 4.5.

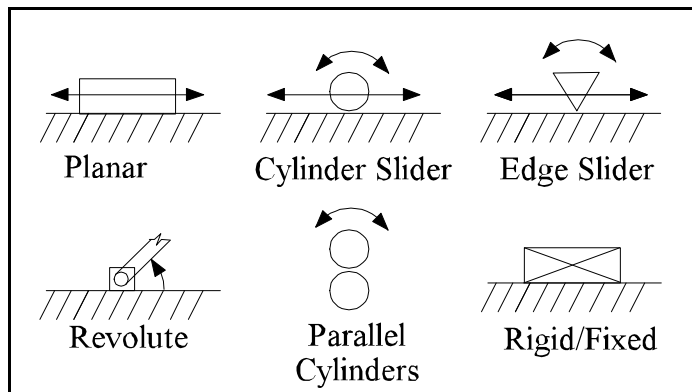


**Figure 4.5** Kinematic joints and their associated degrees of freedom.

The four joints for the stacked blocks are shown in Figure 4.6, represented by symbols added at each location. Orientation of each symbol corresponds to the joint axes and indicates the direction of the degrees of freedom.

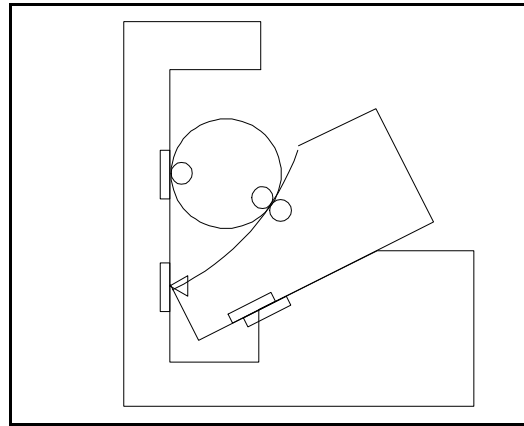


**Figure 4.6** Joints for the stacked blocks assembly.

#### 4.2.4 Skeleton Diagrams

Skeleton diagrams for assemblies trace the paths between joints and part/feature DRFs. In effect, the skeleton diagram defines the critical dimensions of the assembly. In the systematic procedure this step is often combined with the next step, creating the vector loops.

#### 4.2.5 Creating Vector Loops

Vectors are placed on the assembly using the network graph as a guide. The placement of these vectors is governed by a set of rules, given below.

1. The set of loops must pass through every part and every joint in the assembly.
2. As a vector loop traverses a part, it must pass through the DRF of the part.
3. No single loop may pass through a part or joint more than once, but it may start and end in the same part.

4. There must be enough vector loops to solve for all of the kinematic variables - one loop for every three variables in a 2-D assembly..
5. Paths of vector loops must follow part dimensions or kinematic variables.

Additional rules define the path of vectors passing through various joints.

1. For a cylindrical slider joint, either the incoming or outgoing vector must be normal to the sliding plane and end at the center of the cylinder.
2. For joints having a sliding plane (planar, cylindrical slider or edge slider), either the incoming or outgoing vector must lie in the sliding plane.
3. For parallel cylinder joints (two parallel cylinders in contact), the path through the joint must start at the center of one cylinder and end at the center of the mating cylinder, passing through the contact point.

Applying these rules to the stacked block assembly yields three vector loops, shown in Figure 4.7.

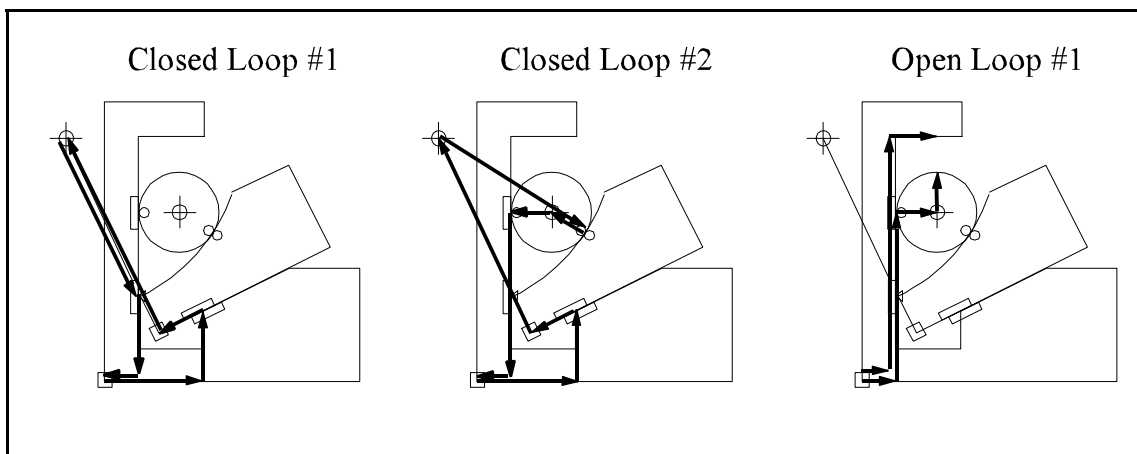


**Figure 4.7** Vector loops for the stacked blocks problem.

### 4.3 Developing the Equivalent Variational Mechanism from the Vector Loops

With a complete set of vector loops that apply both to the tolerance analysis and the kinematic analysis, it is now possible to start adding the necessary elements to create an EVM.

#### 4.3.1 Skeleton diagram

The three loops may be combined to form a single skeleton diagram of the EVM. Each vector in the loops represent an element in the skeleton diagram. Each element in the skeleton diagram represents a link in the EVM. Figure 4.8 shows the resulting skeleton diagram without any kinematic joints. Every dimension that contributes to assembly variation is represented by a link. Dimensions appearing in more than one loop are represented by a single link in the EVM. Overlapping links have been shown slightly offset for clarity. Additional joints must be added to each link to complete the equivalent variational mechanism in order to introduce dimensional variation. Additional elements are described in the following sections.

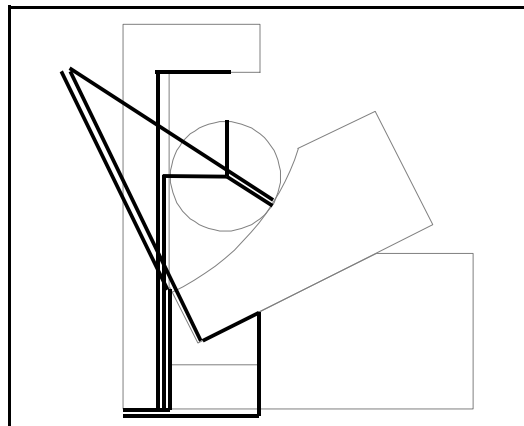


**Figure 4.8** Skeleton diagram for the equivalent variational mechanism.

### 4.3.2 Network Diagram (Equivalent joints)

Links of an equivalent variational mechanism represent the geometry of the system while the joints represent the way the geometry varies. We previously used a network diagram to determine the path of vectors through the joints in the assembly. We now refer back to the network diagram to determine the placement of equivalent joints.

There are two types of joints that must be represented in the equivalent variational mechanism, equivalent kinematic joints, and equivalent independent joints. Velocities at equivalent kinematic joints are unknown and represent the dependent variations in the tolerance analysis. Independent variations are represented as velocities applied to the independent joints of the EVM.

### 4.3.3 Independent Variations

The next step is to include all of the independent dimensional variation sources in the EVM. Independent variations considered in this thesis are of two types: linear and angular dimensional variations. Each link represents a dimension in the assembly. Linear variations of these dimensions are represented by a velocity applied to a translational joint between the ends of the link, as seen in figure 4.9.

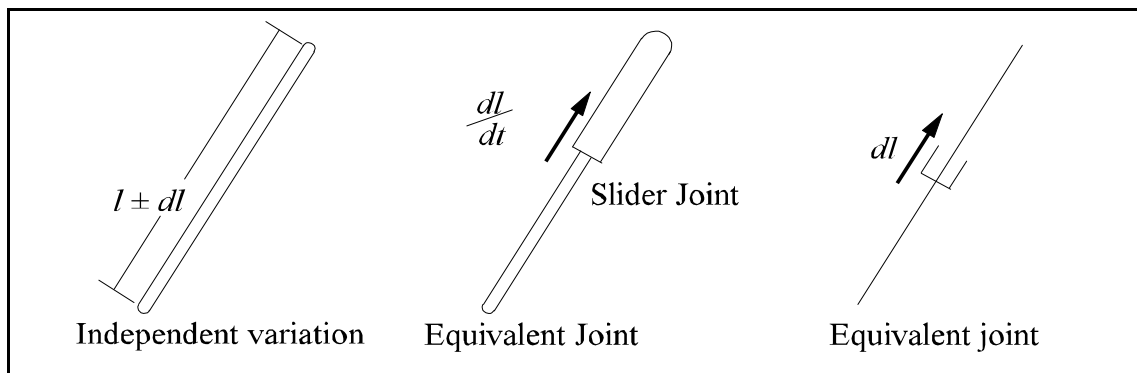


**Figure 4.9** Equivalent joints used to represent independent length variations

Angular variations between links are represented by an input velocity applied to a revolute joint. When dealing with mechanisms it is possible to have an independent angular variation located at an existing pin joint, such as when there is uncertainty in the initial angular position of the driver link of a four-bar mechanism. In these cases the angular variation is applied as a velocity to the existing pin joint since existing pin joints are not replaced in the equivalent variational mechanism.

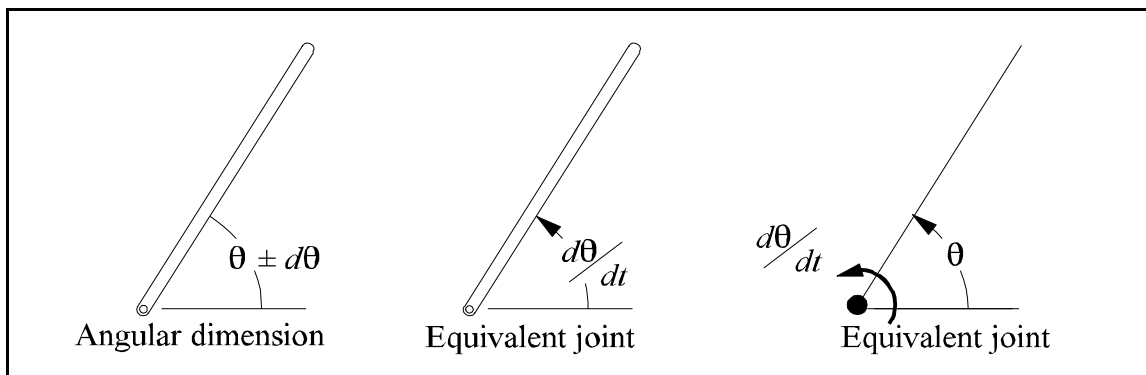


**Figure 4.10** Equivalent joints used to represent independent angular variations

Figure 4.11 shows the addition of joints in the equivalent variational mechanism corresponding to linear and angular dimension variations.

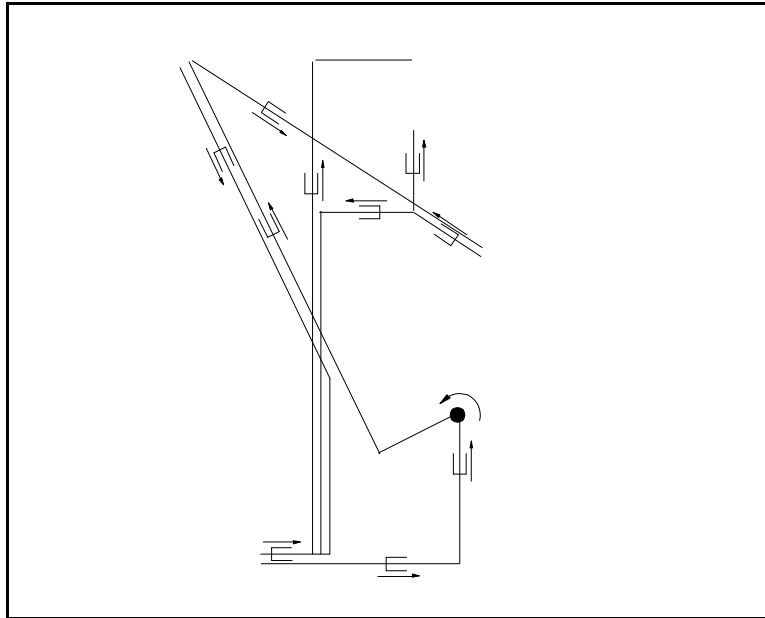


**Figure 4.11** Adding joints representing independent variations for the stacked blocks assembly.

In the stacked block assembly there are three vectors representing radii of the Cylinder. All three are controlled by the same dimension. Similarly, there are two large radii on the Block which are controlled by a single dimension. Velocities applied to slider joints in links controlled by the same dimension must have the same magnitude. Arrows in the figure represent input velocities applied to the joints. Each independent variation can be mapped as a velocity. Resulting dependent velocities can be related to a single case tolerance analysis solution by scaling the input velocities to be equal to the tolerances of the component dimensions. Using the equivalence between tolerance sensitivities and the Jacobian of the kinematic solution allows the calculation of statistical assembly tolerances.

#### 4.3.4 Equivalent Kinematic Joints

Revolute and rigid joints are identical in EVMs and assemblies. All of the other kinematic joints can be represented by equivalent joints in the EVM. This section describes each of these equivalent joints.

### Planar Joint

The planar joint allows a sliding degree of freedom between two parts. This sliding degree of freedom is represented as a translational joint on the link that is in the sliding plane. The point of contact for this joint is modeled as a revolute joint, allowing representation of independent rotational variations at this joint. A rotational velocity of zero is applied to the joint when there is no rotational variation, creating a rotationally rigid joint at the point of contact. Otherwise, as in the case of the stacked blocks, the rotational variation is represented by the non-zero velocity applied to the revolute joint.

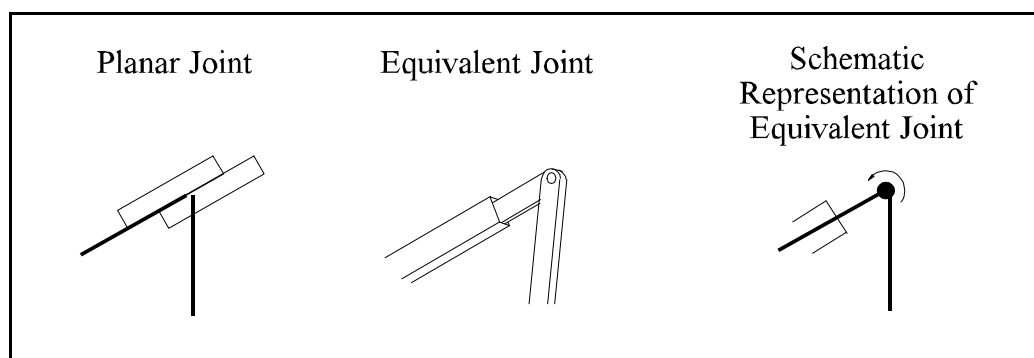


**Figure 4.12** The planar joint.

### Cylindrical Slider

The cylindrical slider joint allows two degrees of freedom, translational and rotational. These degrees of freedom combine to allow three types of motion: pure sliding (no rotation), rolling without slipping (rotation and translation), and rolling without translating (rotation about the center of curvature with no translation). Pure sliding, and

rolling without slipping both cause the point of contact to translate in the sliding plane, represented by a translational joint in the EVM. In both cases, however, there is no relative rotation between the point of contact and the rotational DRF, allowing the point of contact to be represented as a fixed joint. Translation of the contact point may cause relative rotations between the vectors passing through the circular DRF. This variation is represented by a revolute joint at the DRF.

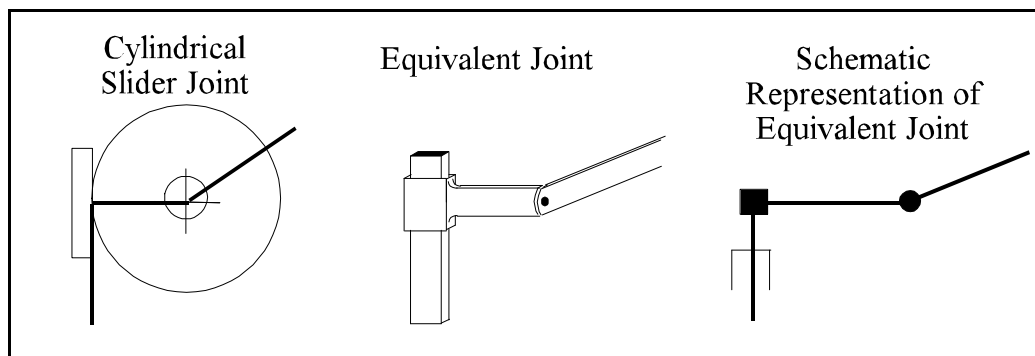


**Figure 4.13** The equivalent joint for the cylinder slider

It should be noted that the slider and revolute joints in this case represent kinematic adjustments rather than dimensional variations. Velocities at these joints are output velocities corresponding to assembly variations.

### **Edge slider**

The edge slider has two degrees of freedom, translation and rotational. The rotational degree of freedom is modeled as a pin joint at the point of contact. The translational degree of freedom is modeled as a slider joint with its degree of freedom in the sliding direction of the kinematic joint. Both degrees of freedom are assembly variables, and are solved for in the kinematic analysis.

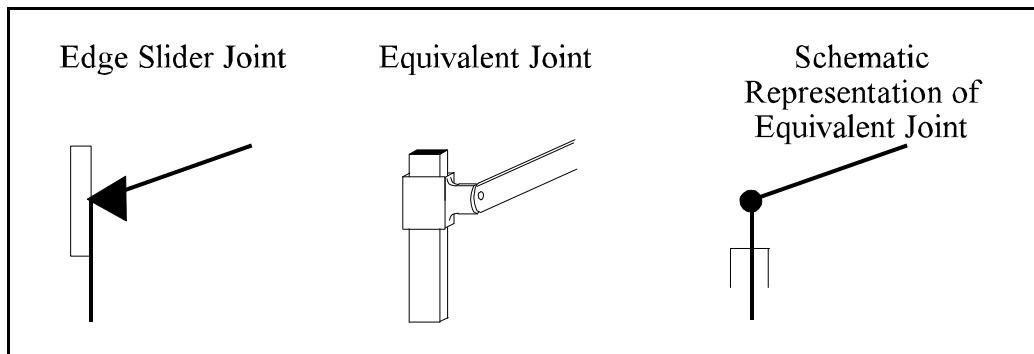


**Figure 4.14** The equivalent joint for the edge slider

**Parallel Cylinders**

The parallel cylinders joint has only one degree of freedom, rotation about the parts center. An equivalent joint is proposed in Figure 4.15. Translational joints are usually found in each link, allowing the pinned ends to rotate around each other in a manner other than circular. The fixed joint keeps the two links colinear.

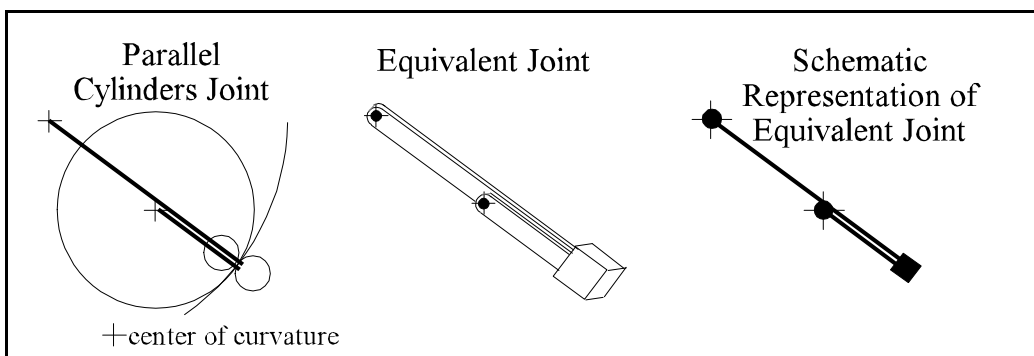


**Figure 4.15** Equivalent joints for the parallel cylinders

Figure 4.16 shows the EVM for the stacked blocks after the kinematic joints have been replaced with their respective equivalent joints.



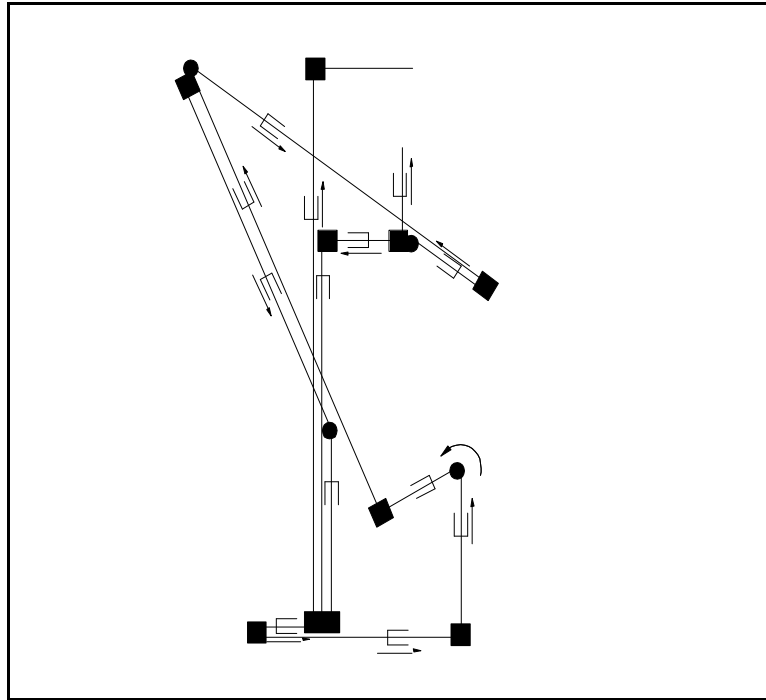


**Figure 4.17** Placement of fixed joints on the stacked blocks assembly.

The EVM for the stacked blocks assembly is now complete. Sensitivities extracted from a kinematic analysis of this mechanism can be used in a tolerance analysis of the stacked blocks.

#### 4.4 Discussion

A step-by-step procedure for the creation of equivalent variational mechanisms (EVMs) has been presented and demonstrated on the stacked blocks assembly. EVMs representing dimensional variation in four common kinematic joints are illustrated in combination with simple length and angle variations. This method provides a comprehensive system for variation analysis applicable to all two-dimensional assemblies. It is suitable for an automated system, linked to a CAD/CAE system.

48

Form variations have not been included.

## **Chapter 5 Application of the TAKS Method Using ADAMS**

Chapters 2 and 3 introduced the TAKS method for tolerance analysis using a four-bar mechanism and one-way clutch as examples. In each case, kinematic and tolerance analysis equations were derived and solved manually. Examples in these chapters demonstrated the relationship between kinematic and tolerance analysis, and validated the use of kinematic sensitivities in tolerance analysis. This chapter focuses on creating an equivalent variational mechanism (EVM) and performing the kinematic analysis of the EVM using the commercial kinematic analysis software ADAMS. Specifically, this chapter describes kinematic modeling techniques as well as methods used for extracting kinematic sensitivities suitable for tolerance analysis. A brief review of the TAKS method is presented, along with an overview of ADAMS. Modeling details are presented using the stacked block assembly, and four bar mechanism as examples.

### **5.1 Summary of the TAKS Method**

The TAKS method can be broken up into three main steps: identify assembly geometry, create and analyze the equivalent variational mechanism (EVM). The first step, identify the geometry, requires the designer to identify the key dimensions that make up the individual parts of the assembly, define reference frames for these dimensions, and sort them as independent and dependent dimensional variation sources. Interactions between parts are identified and categorized using the six kinematic joints presented in Chapter 4.

The next step is to create an EVM. The DRFs, links, and joints defined in the first step are used to create vector loops. Each vector in the loop represents a link in the EVM. The independent variations and joints previously defined in the first step are used to locate and orient the joints in the EVM.

The final step is to perform a kinematic analysis of the EVM. In the second and third chapters we used traditional kinematic techniques (vector loops, vector equations, and matrix methods) to perform the kinematic analysis. In this chapter, we use ADAMS to perform the kinematic analysis.

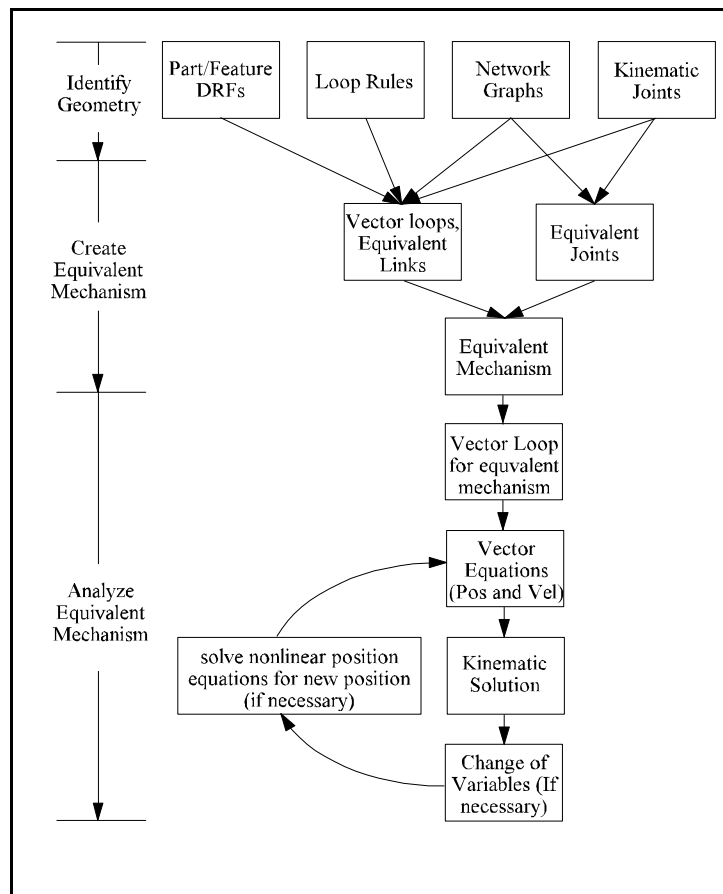


**Figure 5.1** A summary of the TAKS method

## 5.2 Brief Overview of ADAMS

ADAMS stands for Automatic Dynamic Analysis of Mechanical Systems.

ADAMS is a kinematic/dynamic modeling tool which allows the designer to create and test virtual models before building physical prototypes. Using ADAMS, a designer is able to model part geometry, join parts using a variety of joint types, apply motions and forces to the assembly, analyze the kinematics and dynamics of the assembly, animate the motion of the assembly, and track the position and velocity of any point on the assembly.

The basic building block in ADAMS is the marker (Figure 5.2). Markers are local coordinate systems which define points in space, and are used to define the two ends of a link, locate joints between parts, and track positions. Angular variation between links is measured by comparing the relative rotation between two markers defining a joint. Translations are also defined by the relative motion between markers.

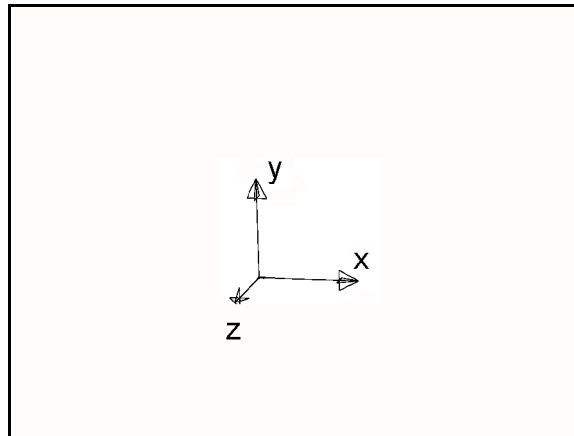


**Figure 5.2** Representation of a marker in ADAMS

ADAMS is fairly easy to use once the use of markers is understood. Several primers [1,2] are available which describe the creation of additional required modeling

elements such as parts, and models. Helpful modeling tips and useful tutorials are also given in these primers. While this chapter will describe the modeling of EVMs in ADAMS a more complete understanding of ADAMS can be obtained by studying its documentation.

### 5.3 Naming Conventions and Other Preparation

As we model the EVM we will be asked to name each part and joint. In addition, ADAMS requires parts to be located and oriented with respect to a global origin. It is helpful to determine and locate all of the parts relative to a global coordinate system, and to name all of the parts and joints before starting the modeling. This contributes to a complete understanding of the model and saves time by avoiding modeling errors. Figure 5.3 shows the location and orientation of all the parts with respect to the global origin located at point *a*.

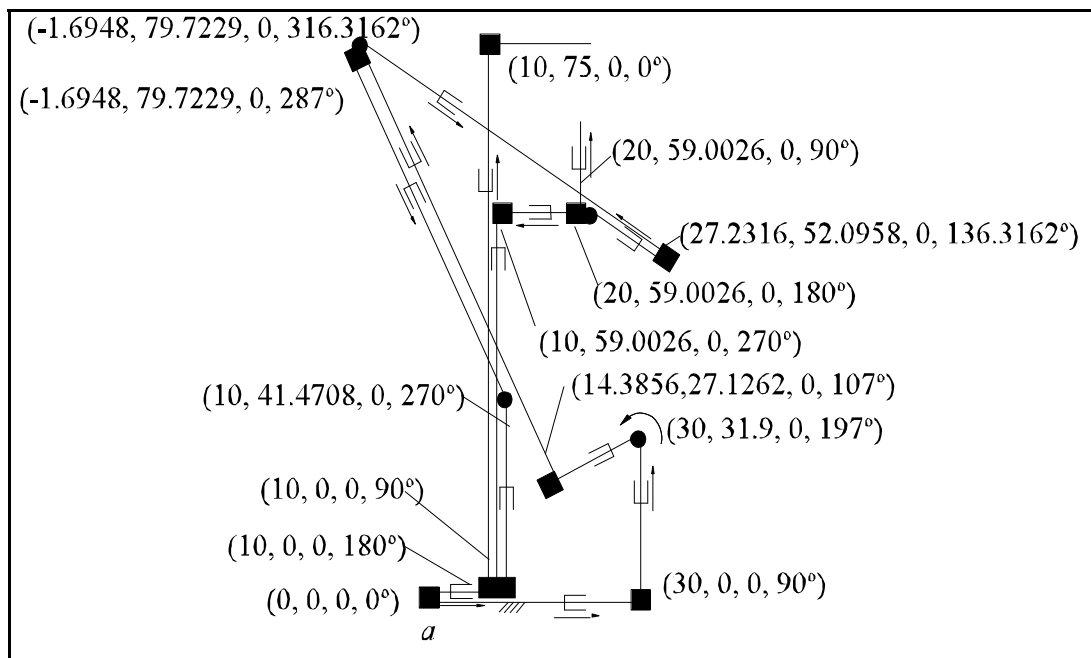


**Figure 5.3** Position and orientation of the links (x, y, z,  $\theta$ ).

All of the parts are named according to the following convention. Links relating to a dimension are given the name of the dimension followed by a number for each additional link controlled by that dimension (Figure 5.4). For example, the two links on either side of a slider joint associated with dimension  $c$  are given the names  $c1$  and  $c2$ . Additional links controlled by dimension  $c$  would be named  $c3$ ,  $c4$ , and so on. The letters  $F$ ,  $P$ ,  $S$ , and  $V$  are used to identify joint types and can not be used as link names. The letter  $J$  indicates a joint and also can't be used as a link name. Joints are named by their type, and by the links that they join. A slider joint in link  $c$  would be name  $SJc$ . A revolute, or pin, joint between links  $c$  and  $d$  would be named  $PJc_d$ , while a fixed joint between the two links would be named  $FJc_d$  (Figure 5.5). Velocities applied to these joints are  $VSc$ , and  $VPc_d$ .

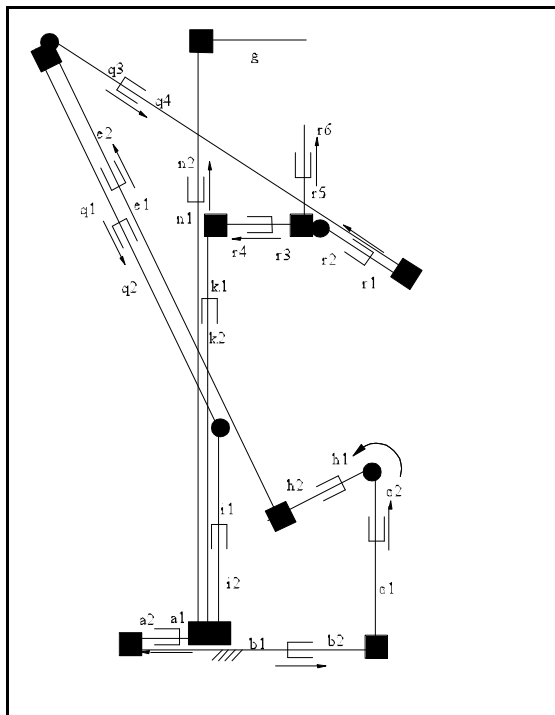


Figure 5.4 Link labels.

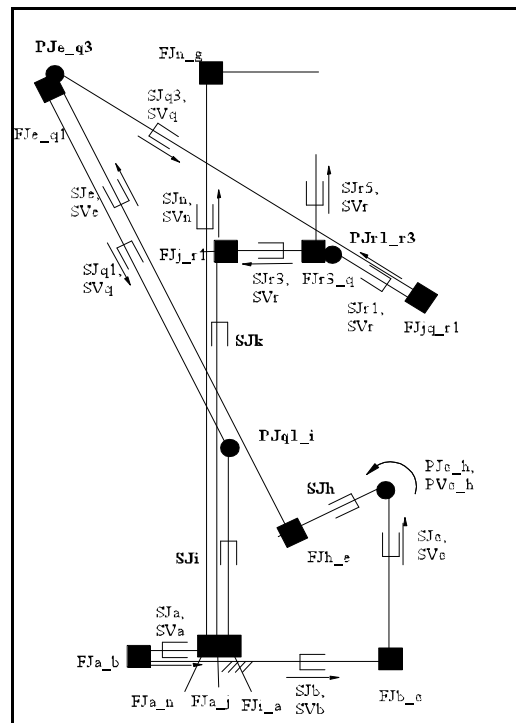
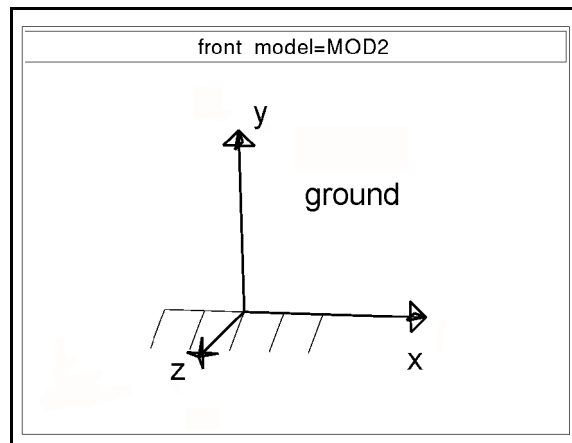


Figure 5.5 Independent and dependent variations

## 5.4 Creation of Mechanism Geometry in ADAMS

Before explaining the creation of geometry in ADAMS it is first necessary to explain some definitions peculiar to ADAMS that could be confusing otherwise. ADAMS defines a model as the global frame of reference with respect to which everything is located. In terms of hierarchy, the model is the parent of all other modeling elements, and is the root of the hierarchal tree. The naming system used in ADAMS reflects this hierarchy with all names of all of the modeling elements separated by a period, starting with the model name. For instance, the complete name of part c belonging to model m is .m.c. A screen capture of a representation of a model in ADAMS is shown in Figure 5.6.



**Figure 5.6** Representation of a model in ADAMS.

Parts are defined as a local coordinate system to which all of the parts children (markers, etc.) are referenced. Again, this is reflected in the naming system used by ADAMS. Marker a1 belonging to part c which is the child of model m is name .m.c.a1. Figure 5.7 shows a screen capture of a part, PAR2, in ADAMS. This part is located with

respect to the model, MOD1.

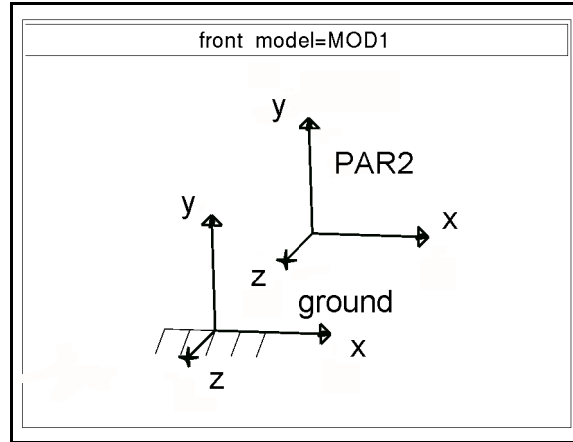


**Figure 5.7** A part in ADAMS, located with respect to the model.

#### 5.4.1 Location of Parts

Parts are defined by creating a local coordinate system to which the geometry of the part can be attached. The part is positioned by locating and orienting the local coordinate system relative to the global system. ADAMS refers to the local coordinate system by the part name. The local part coordinate system can be located anywhere in the model space, even separated from the physical geometry of the part. For links, it is most convenient to locate the local coordinate system of each part at the end of the link, usually the end that was the tail of the vector which defined the link. Orienting the local part coordinate system such that the x axis is coincident with the link allows easy positioning of markers defining the part geometry.

Length variations in links were considered in the EVM by adding a slider joint to

the link, in effect splitting the link into two sub-links. Each of these sub-link must be modeled. The parts for both sub-links are located at the end of the link which is the tail of the vector describing the link. This is done for convenience in locating the slider joint, and is discussed further in following sections.

#### 5.4.2 Markers and Zero Length Links

With the parts defined we can now begin to define geometry. The geometry of the parts is defined by markers. For the links, the ends of each sub-link are defined by markers, making a total of four markers per link. For simplicity, the first three markers are all located at the origin of local part coordinate system. The fourth marker is placed at the far end of the link. The markers are named using the link name, and the markers position on the link. For link  $c$  the marker are named  $c0$ ,  $c1$ ,  $c2$ , and  $c3$ . Marker  $c0$  and  $c1$  form the first sub-link, while markers  $c2$  and  $c3$  form the second sub-link and define the length of the link (Figure 5.9).

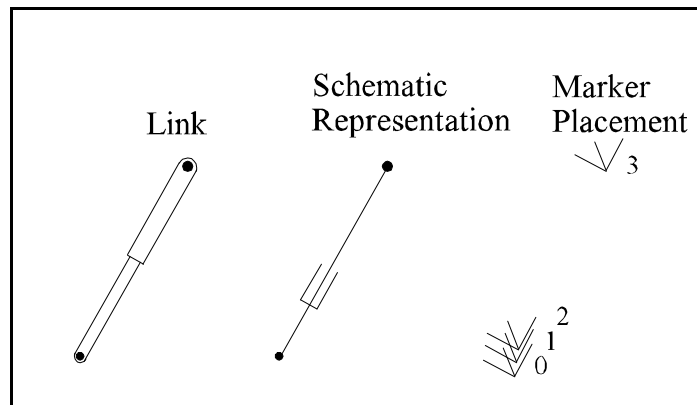


**Figure 5.8** Placement of marker on links with slider joints.

The slider joint is placed between the ends of the two sub-links at markers 1 and 2.

Applying a velocity at this joint causes the ends of the link (0 and 3) to move away from or towards each other. The first sub-link has no length and is known as a zero-length sub-link. Zero-length sub-links are used for convenience in modeling. We could place the slider joint representing length changes of links anywhere in the link, but it is most convenient to locate it at one of the ends of the link. By convention, the joint is always placed at the part origin.

### 5.4.3 Creation of Links

With markers in place defining the geometry of the links we can now create the links themselves. ADAMS allows the creation of links by defining the two markers at the ends of the links. The links for the EVM for the stacked blocks assembly are shown in Figure 5.9.

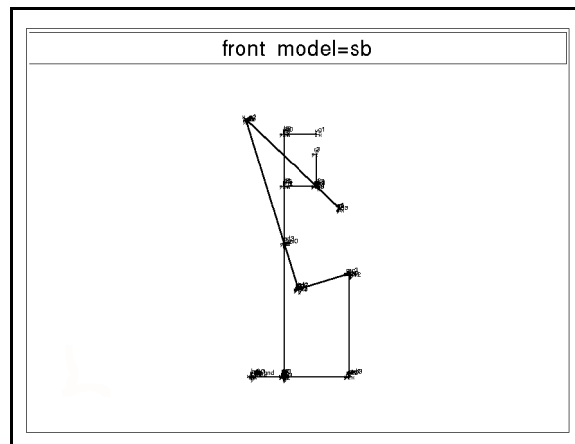


**Figure 5.9** The links of the EVM for the stacked blocks assembly.

### 5.4.4 Creation of Joints

ADAMS creates joints by constraining appropriate degrees of freedom of the markers defining the joint. There is a library of common kinematic joints in ADAMS which can be placed in the model. Of these, only the translational, revolute, and fixed joints were used in EVMs. Translational joints are most conveniently placed using the coordinates and orientation of the joints relative to the local part reference frame. The joint is placed at the parts origin, since this is the location between the two sub-links. The joint must be rotated (90, 90, 0) during its placement. Figure 5.10 shows the slider joint between  $b1$  and  $b2$  for the stacked blocks assembly.

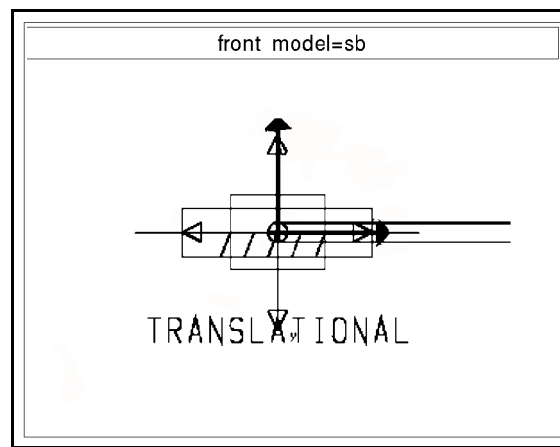
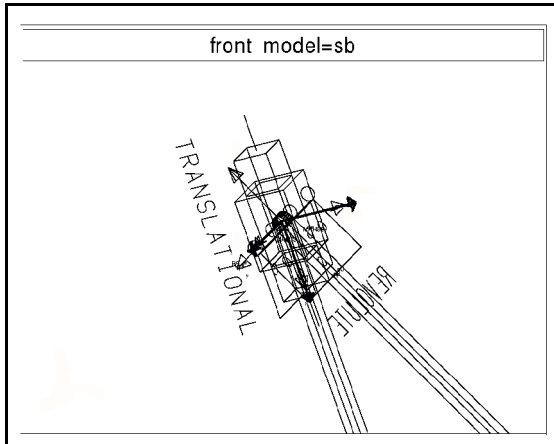


**Figure 5.10** Representation of a translational joint in ADAMS.

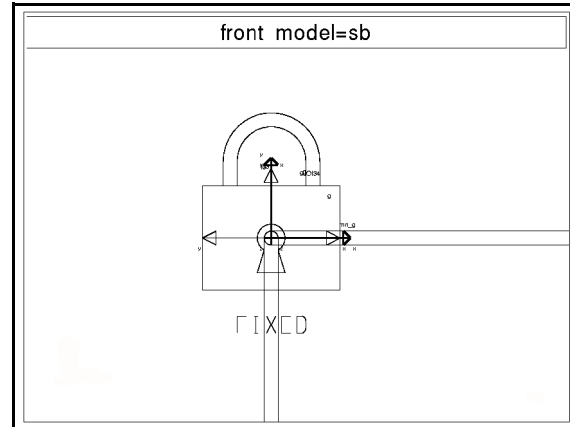
Revolute and fixed joints are most easily placed using the markers which define the ends of the links to be joined. The z-axis of the markers must always be coincident for both joint types. The x and y axes must be coincident for revolute joints with applied angular velocities (independent angular variation sources) and fixed joints.

Figure 5.11 shows the pin joint between  $e2$  and  $q3$ , while Figure 5.12 shows the

fixed joint between  $n2$  and  $g$ .



**Figure 5.11** A representation of a revolute joint in ADAMS.



**Figure 5.12** Representation of a fixed joint in ADAMS.

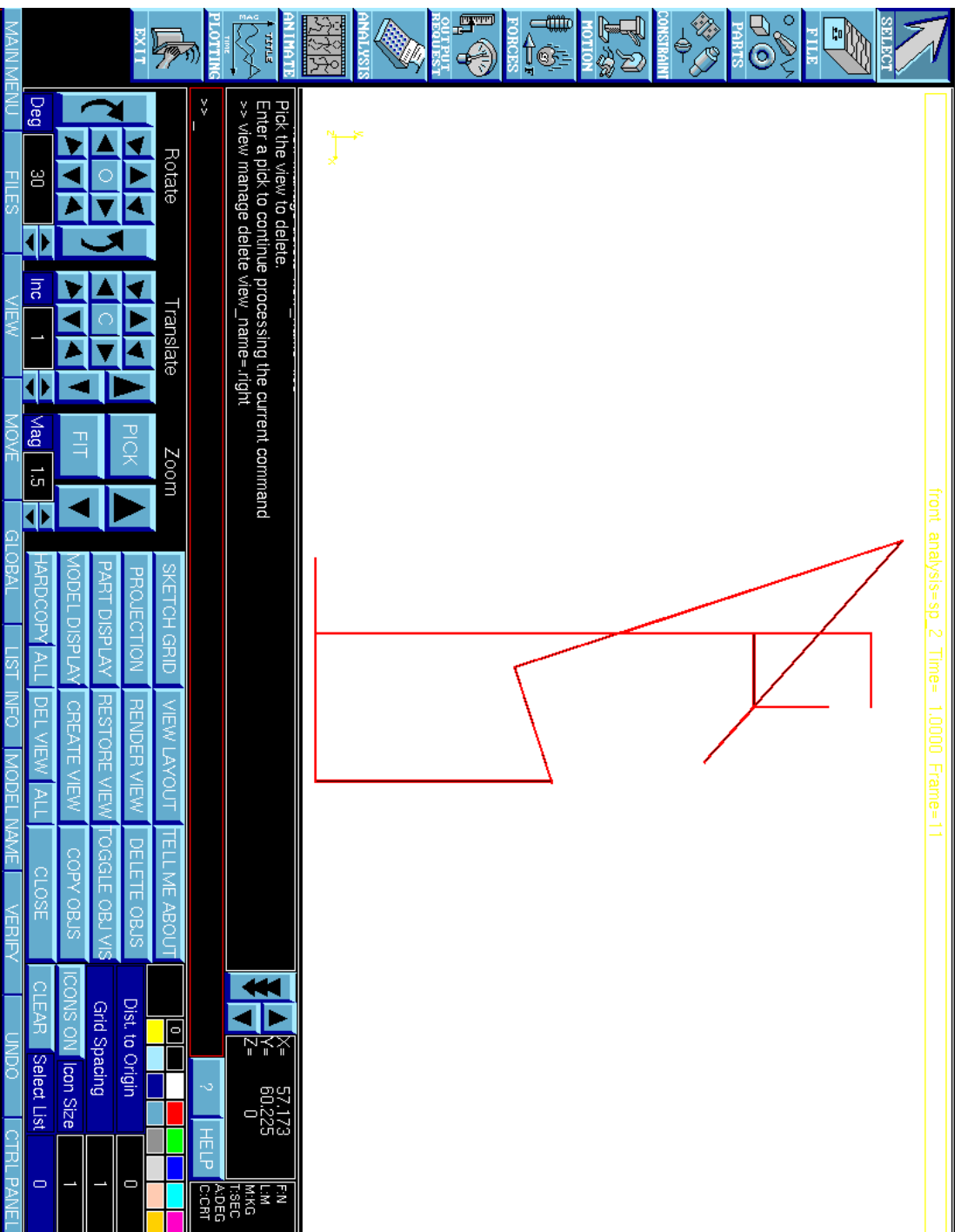
In ADAMS, the symbol for a revolute joint is a hinge, and the symbol for a fixed joint is a padlock.

### 5.5 Adding Motions on Joints

Input motions may be applied to joints as displacements, velocities, or accelerations. To correctly represent tolerances, motions must be applied as velocities. Velocities are applied to all independent joints (excluding fixed joints). A single case tolerance solution can be obtained by setting the magnitude of each of the velocities equal to its corresponding tolerance value. Sensitivities must be extracted for statistical tolerance analysis. The extraction of sensitivities is explained in section 5.6

Adding motions to the joints completes the modeling of the EVM in ADAMS.

Figure 5.13 shows a screen capture of the completed model of the EVM for the stacked blocks assembly.



99 **Figure 5.13** The completed model in ADAMS. Joint icons have been turned off for clarity.

## 5.6 Output Requests

The user determines the results to be output by ADAMS by submitting output requests. The requests are based on markers. For instance, in the stacked blocks problem an output request was made to track the velocity between the marker at the end of links  $g$  and  $r6$ , the critical gap dimension defined for the stacked blocks. The output request gives results relative to the two markers associated with the request, eliminating any need for performing absolute-to-relative transformations on the results. However, the resulting gap velocity is not directly related to the variation in the gap. To estimate the variation either statistically or by worst case, requires the sensitivities of the gap to each of the independent dimensions.

## 5.7 Extracting Sensitivities from Static Assemblies

All of the sensitivity information that is needed is stored in the jacobian matrix calculated for each analysis step. However, ADAMS does not store any labels associated with the jacobian matrix, so specialized code must be developed to identify and extract the desired sensitivities. It is still possible to extract the sensitivities using an alternative method. Sensitivities describe the individual contribution of each independent variation to the overall variation. Using ADAMS, it is possible to isolate the contribution of each independent variable by setting the velocity of the variable to a unit input with all other velocities zero (except where more than one velocity is controlled by the same dimension). The resulting output velocity represents the sensitivity corresponding to the input velocity. Repeating this process for each independent variable provides a method for determining the kinematic sensitivity matrix.

Table 5.1 shows the sensitivities of the critical dimension, the gap, with respect to each independent variable. The resulting sensitivities can be used to form a root sum squares expression used for a statistical tolerance analysis of the stacked block assembly, as presented in Chapters 2 and 3.

**Table 5.1** Open loop sensitivities for the stacked blocks assembly.

	<i>a</i>	<i>b</i>	<i>c</i>	<i>e</i>	<i>n</i>	<i>g</i>	<i>q</i>	<i>r</i>	<i>theta</i>
dgap	-0.306	0.306	-1	-1.046	1	0	1.231	-3.495	-0.197

In this case, the sensitivity matrix is a 1 x 7 matrix, since there was only one critical assembly feature. Sensitivities for the closed loop kinematic variables can be obtained by making corresponding output requests before performing the analysis. Each additional assembly feature requested adds one more row to the sensitivity matrix. Solving the system for a unity input velocity yields a full column of the sensitivity matrix, so you still only need to perform the analysis as many times as there are independent dimension variables, in this case, seven times.

## 5.8 Extracting Sensitivities for Mechanisms

Extracting sensitivities is somewhat more complicated for mechanisms, since the sensitivities must be calculated for the full range of motion of the mechanism. A new sensitivity matrix must be calculated for each new position of the mechanism, forming a stack of sensitivity matrices with each layer in the stack representing a new position of the mechanism. Earlier, in Chapter 2, a tolerance analysis for the assembly position of a crank-rocker four-bar mechanism was presented. We will use this same four-bar

mechanism to demonstrate the extraction of the kinematic sensitivities for the full range of motion of the mechanism, using ADAMS.

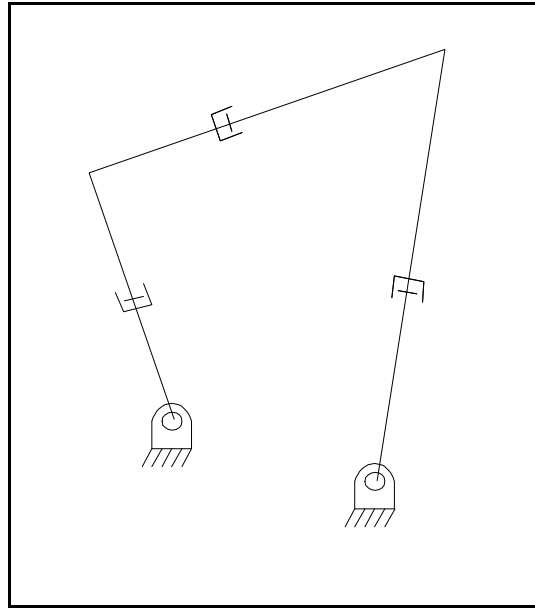


**Figure 5.14** Equivalent variational mechanism for the four-bar linkage.

The overall motion of the mechanism can be split up into two categories : the small kinematic adjustments caused by dimensional variations, and the larger kinematic motion (the overall motion without the kinematic adjustments) due to prescribed motion of the input crank. For the four-bar mechanism, kinematic motion results from applying a velocity to the input link, while kinematic adjustments are caused by motions applied to the slider joints. The input velocity on the driver link is necessary to rotate the mechanism through its range of motion, but when there are inputs on both the driver link and slider joints, resulting sensitivities are the sum of the contributions of each input. The contribution due to the input velocity on the driver link can be found by performing the

analysis with just this velocity applied to the mechanism. Sensitivities due to velocities applied to each slider joint can be found by reworking the analysis with a unit velocity applied to each slider joint (one at a time), and subtracting the portion of the sensitivities due to the input angular velocity.

### 5.8.1 Techniques for Automatically Resetting Nominal Lengths

For static assemblies we were only worried about the initial position (the nominal position of the assembly) so we didn't care what position the EVM ended in. For mechanisms however, the links must all be at their nominal lengths, and nominal positions for each new position of the mechanism. Velocities applied to slider joints must be able to bring the link back to its nominal size for each new position of the mechanism. This can be accomplished by applying the velocity as an oscillating function of time. The cosine function is ideal, since it has a magnitude of one at the beginning of each new period, when the initial time is equal to zero (see Figure 5.15).

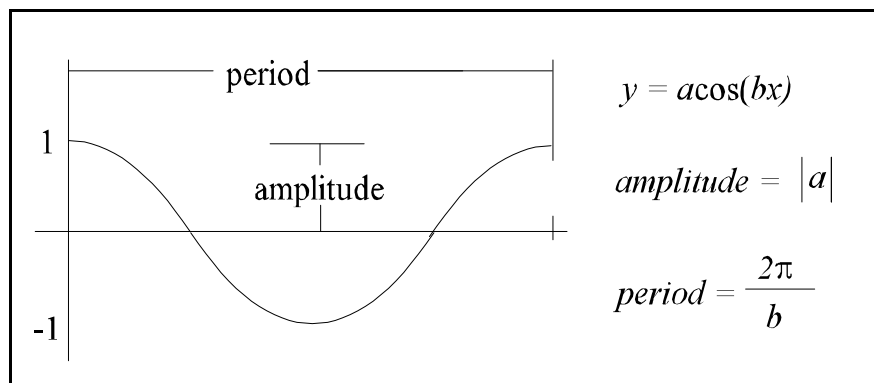


**Figure 5.15** The cosine function.

A joint then can always be made to return to its original position at each time step by choosing an appropriate value for  $b$ . Each new time step in the analysis represents a

new position of the mechanism, and the period should be chosen to match the time-step size. For instance, if the analysis is set with a time step size of one-tenth of a second, the links in the mechanism must be at their nominal positions every one-tenth of a second. This is accomplished by setting the period of the function controlling the slider velocity to be equal to one-tenth of a second, which occurs when  $b = 20B = 62.8319$ . The magnitude of the slider velocity at this point is equal to the amplitude, which should be set as a unit value.

The period controls the resolution of the analysis, the number of steps per revolution. For instance, setting the period as one second causes the link to return to its nominal size every second, and provides 360 sensitivity matrices for each full rotation of the mechanism. Reducing the period to .1 seconds creates a much finer resolution - providing 3600 stacks in the data. It is often convenient to set the period equal to one for the initial analysis, in which case  $b$  is equal to  $2B$ . Any necessary refinements can then be made using a smaller period.

### **5.8.2 Integration Error**

There is some accumulation of error in this process. Analysis performed on a four bar with complete rotation demonstrates this error. The starting and ending points of the four-bar mechanism should have the same sensitivities, since they are really the same position. With a period of one second, sensitivity results drifted as far as ten percent between starting and ending points. This error is due to the numerical processes used by ADAMS to calculate each new position of the mechanism for each time step, and can be reduced by decreasing the time step size used in the analysis or by restarting at a new

initial position. Coarse analysis can be used to determine the critical position of the mechanism and fine analysis to determine the maximum variation more accurately.

Figure 5.16 shows the sensitivities for the four-bar mechanism shown in chapter two. The sensitivities at the beginning match the sensitivities calculated in chapter 2.

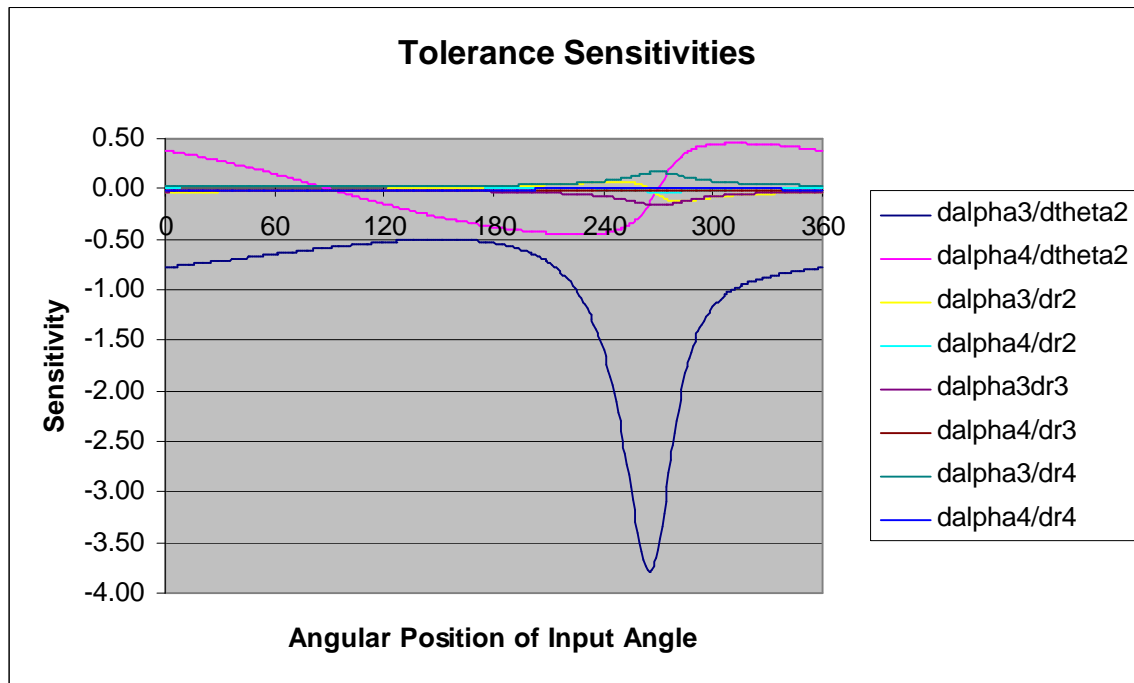


**Figure 5.16** Tolerance sensitivities for the full rotation of the four-bar mechanism.

Note that the tolerance sensitivities generally have a greater magnitude at  $270^\circ$ , in some cases nearly 400 percent greater. This is the critical position of the four-bar mechanism which should be used to make design decisions.

The sensitivities can be used to form root sum square expressions in a statistical tolerance analysis. Resulting statistical variations are shown in Figure 5.17. It is obvious that the assembly position is not the critical position for tolerances. Tolerances should be assigned based on the sensitivities at the critical position,  $270^\circ$  rotation of the input angle.

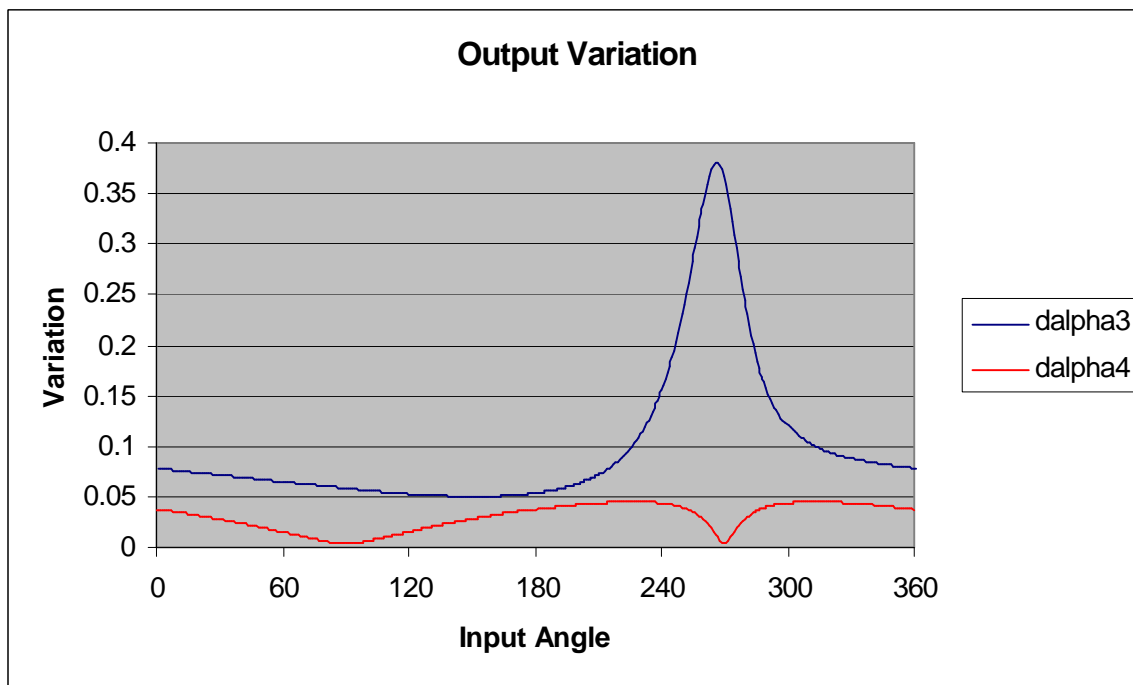


**Figure 5.17** Statistical variation for the full rotation of the four-bar mechanism.

### 5.9 Degrees of Freedom Problems in the Equivalent Mechanism.

There are some degree of freedom problems arising from using two-dimensional joints in three-dimensional modeling space. We can see this with the four-bar mechanism. A Gruebler count of the four-bar mechanism indicates 0 degrees of freedom using two dimensional techniques, but -3 degrees of freedom when using 3-D techniques. Table 5.2 demonstrates the Gruebler count in both two and three dimensions.

**Table 5.2** Gruebler count of the four-bar mechanism in both two and three dimensions.

	2d	3d
links (7)	$3*7 = 21$	$6*7 = 42$
ground link	$-3 = 18$	$-6 = 36$
Revolute Joints (4)	$-4*2 = 10$	$-4*5 = 16$
Translational Joints (3)	$-3*2 = 4$	$-3*5 = 1$
Motions (4)	$-4 = \mathbf{0}$	$-4 = \mathbf{-3}$

The four-bar is over-constrained when modeled in three-dimensional space using two-dimensional joints. This can cause convergence problems in the analysis.

Convergence problems can be avoided by replacing the revolute joints between the driver and coupler, and coupler and follower with a spherical joint and universal joint.

Models of other EVMs end up with a positive Gruebler count, meaning an under-constrained mechanism. The quick fix in these cases is to apply masses to each of the links and use a dynamic analysis instead of kinematic.

## 5.10 Recommended Modifications for ADAMS

The TAKS method is ideally suited for application using ADAMS software. Modifications made to ADAMS (either directly to ADAMS or in the form of add-on software) would speed up the process and make it easier to apply.

### 5.10.1 Automated Placement of Sub-Link Equivalent Joints.

A large portion of modeling time is spent creating each sub-link and joining them with slider joints. This is a process that could be automated. The designer would be required to model the links representing dimensions in the assembly, then specify which of

these dimensions are allowed to vary. ADAMS could then build the zero-length links and place slider joints between the links.

Another process well suited for automation is the placement of the equivalent kinematic joints. The designer could specify two links then choose the type of joint to place and allow ADAMS to place and orient the equivalent joint. Figure 5.17 recaps each of the kinematic joints used in traditional tolerance analysis, along with the replacement joints used in the EVM.

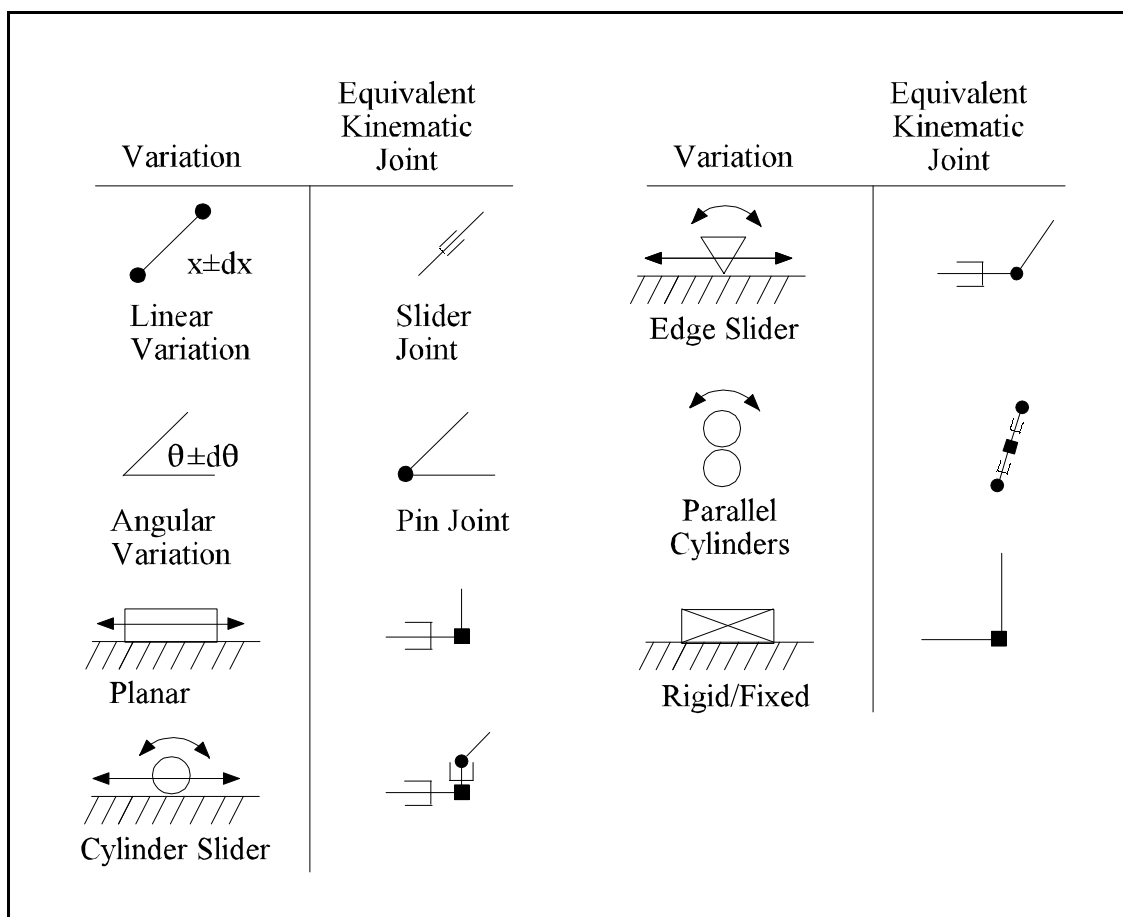


**Figure 5.18** Summary of equivalent variational joints.

### **5.10.2 Integrating Solid Modeling Packages**

Another change in ADAMS that would benefit the modeling process would be designing a filter to bring in existing solid models of assemblies. Ideally, solid models of assemblies would be used to help create an EVM for the assembly. Superimposed over the EVM, solid models could also serve as a valuable verification tool.

### **5.10.3 Automation of the Extraction of the Kinematic Sensitivities.**

The extraction of sensitivities requires applying a unit velocity to each independent joint, one at a time. This process can be tedious, especially with appreciable numbers of independent joints and with multiple position mechanism analysis. Ideally, the sensitivities would be extracted directly from the Jacobian matrix stored for each time step of the analysis, but this would require specialized code developed by the programmers of ADAMS.

Even without the specialized code developed by ADAMS it would be possible to automate the method for extracting sensitivities described above. Macros could be developed which automatically set up and perform each of the analysis required to extract the sensitivities. Mathematical operations such as subtracting the input angle sensitivities would be performed automatically as part of this macro.

### **5.10.4 Automated RSS Calculation**

The calculation of statistical assembly variances is straightforward once sensitivities are known. This could be easily integrated into ADAMS. Results could be graphically and numerically displayed.

### **5.10.5 User Interface**

Key to the implementation of these changes will be a well thought out user interface. The tolerance interface should naturally lead a user through the necessary steps in building and analyzing EVMs.



## **Chapter 6 Conclusions and Recommendations**

The development of a new method for tolerance analysis called the TAKS method (Tolerance Analysis using Kinematic Sensitivities) has been presented. The method is based on an analogy between kinematic analysis and variation analysis, which permits tolerance analysis of an assembly to be performed by inserting dimensional variations into a kinematic model. This chapter summarizes the specific contributions made and makes recommendations for future research.

### **6.1 Contributions**

1. The equivalence of kinematic sensitivities and tolerance sensitivities has been demonstrated and appropriate transformations to obtain one from the other have been derived.
2. When applied to planar mechanisms, the TAKS method can be used to derive the tolerance sensitivities at each position over the full range of motion of the mechanism.
3. It was demonstrated that tolerance analysis of a static assembly can be performed using kinematic analysis by representing the assembly as a kinematic mechanism.
4. A systematic method for creating and analyzing equivalent variational mechanisms (EVMs) of both static assemblies and planar mechanisms was developed.
5. A set of equivalent 2-D kinematic joints, which include dimensional variations, was presented as a modeling tool.

6. In addition to hand worked examples, the TAKS method was demonstrated using the commercial kinematic software, ADAMS. Modeling issues such as zero-length links and degree of freedom problems were described.
7. A method for extracting the kinematic sensitivities from the ADAMS model was presented.
8. Modeling techniques were described which cause the links in the EVM to return to their nominal position for each time step, and which remove the extra portion of calculated sensitivities due to the kinematic motion of the mechanism.
9. Recommendations were given for integrating/automating major components of variational modeling and analysis with a commercial kinematic software.

## **6.2 Recommendations**

This research has focused on the relationship between the first kinematic derivative, velocity, and the first statistical moment, variance. This lays the groundwork for the investigation of the relationship between the second and third kinematic derivatives, acceleration and jerk, and the second and third statistical moments, skewness and kurtosis. The ability to use a kinematic modeling package to derive the skewness and kurtosis of an assembly would be a valuable tool and is a primary area of research currently being pursued. In addition to research in this area, the following areas deserve additional research.

### **6.2.1 Integration with Commercial Kinematics CAD Applications**

Integration of tolerance analysis with commercial kinematic CAD applications can readily be achieved, using the methods and modeling techniques presented.

For example, ADAMS provides several utilities which allow for user-based customization. Recommended changes in ADAMS presented in chapter 5 could be investigated for implementation. This would reduce the time required to model and analyze equivalent mechanisms.

### **6.2.2 Extension into Three-Dimensional Assemblies and Mechanisms.**

In its present form the TAKS method applies only to two-dimensional assemblies and planar mechanisms. Other CATS research has developed three-dimensional methods which should be incorporated into the TAKS method.

### **6.2.3 Degree of Freedom Problems**

It was mentioned in chapter 5 that equivalent mechanisms with zero degrees of freedom in 2-D become over-constrained when modeled in 3-D modeling space. This has caused some difficulty in the modeling and analysis of equivalent mechanisms. It would be valuable to be able to determine before modeling an equivalent mechanism on ADAMS what degree of freedom problems may arise and how to fix them. This would eliminate reworking the model to overcome the degree of freedom problems, saving time.

### **6.2.4 Inclusion of Form Tolerances in this Method**

In its present form the TAKS method does not consider form variations, which can be a significant variation source. Again, previous CATS research has successfully included form variation in computer-aided tolerance analysis. This research could extend the TAKS method to allow for the inclusion of form variations in the analysis.

### **6.3 Conclusion**

This is a new area with significant potential. Developing the analogy between kinematic models and variational models has potential of increasing the efficiency of variational modeling and statistical analysis. Integration with commercial kinematics CAD packages will be an important enhancement to mechanism design.

## Appendix A

The transformation represented by the first element in the first row requires an additional redundant equation to be added to the system in order to get the desired transformation.

The additional equation is  $\mathbf{w}_2 = \mathbf{w}_2$  making the system from Equation 2.15:

$$\begin{Bmatrix} \mathbf{w}_3 \\ \mathbf{w}_4 \\ \mathbf{w}_2 \end{Bmatrix} = \begin{bmatrix} J_{1,1} & J_{1,2} & J_{1,3} & J_{1,4} & J_{1,5} \\ J_{2,1} & J_{1,2} & J_{1,3} & J_{1,4} & J_{1,5} \\ 1 & 0 & 0 & 0 & 0 \end{bmatrix} \begin{Bmatrix} \dot{r}_1 \\ \dot{r}_2 \\ \dot{r}_3 \\ \dot{r}_4 \end{Bmatrix} \quad (\text{A.1})$$

Transformation matrix [T]:

$$[T] = \begin{bmatrix} 1 & 0 & -1 \\ -1 & 1 & 0 \\ 0 & 0 & 1 \end{bmatrix} \quad (\text{A.2})$$

is used to perform the row operations on equation 26 yielding the kinematic sensitivity matrix [K] .

$$\begin{aligned} [K] &= \begin{bmatrix} 1 & 0 & -1 \\ -1 & 1 & 0 \\ 0 & 0 & 1 \end{bmatrix} \begin{bmatrix} J_{1,1} & J_{1,2} & J_{1,3} & J_{1,4} & J_{1,5} \\ J_{2,1} & J_{2,2} & J_{2,3} & J_{2,4} & J_{2,5} \\ 1 & 0 & 0 & 0 & 0 \end{bmatrix} \\ &= \begin{bmatrix} J_{1,1} - 1 & J_{1,2} & J_{1,3} & J_{1,4} & -J_{1,5} \\ J_{2,1} - J_{1,1} & J_{2,2} - J_{1,2} & J_{2,3} - J_{1,3} & J_{2,4} - J_{1,4} & J_{2,5} - J_{1,5} \\ 1 & 0 & 0 & 0 & 0 \end{bmatrix} \end{aligned} \quad (\text{A.3})$$

Removing the redundant row and writing the complete equation:

$$\begin{Bmatrix} d\mathbf{a}_3 \\ d\mathbf{a}_4 \end{Bmatrix} = \begin{bmatrix} J_{1,1} - 1 & J_{1,2} & J_{1,3} & J_{1,4} & J_{1,5} \\ J_{2,1} - J_{1,1} & J_{2,2} - J_{1,2} & J_{2,3} - J_{1,3} & J_{2,4} - J_{1,4} & J_{2,5} - J_{1,5} \end{bmatrix} \begin{Bmatrix} d\mathbf{q}_2 \\ dr_1 \\ dr_2 \\ dr_3 \\ dr_4 \end{Bmatrix} \quad (\text{A.4})$$

which is the tolerance variations  $d''_3$  and  $d''_4$  found using kinematic sensitivities.



## References

1. *ADAMS/View Menus and Panels Interface Primer*, Version 8.0 (1994), Mechanical Dynamics, Ann Arbor.
2. *ADAMS/View Icon Interface Primer*, Version 8.0 (1994), Mechanical Dynamics, Ann Arbor.
3. Carr, Charles David, 1993, *A Comprehensive Method for Specifying Tolerance Requirements for Assemblies*, Masters Thesis, Brigham Young University.
4. Chun, Ki S., 1998, *Development of Two-Dimensional Tolerance Modeling Methods for CAD Systems*, Masters Thesis, Brigham Young University.
5. Faik, S. and Erdman, A.G., 1991, "Sensitivity Distribution in the Synthesis Solution Space of Four Bar Linkage," *Journal of Mechanical Design*, vol.113, pp.3-9.
6. Fenton, R.G., Cleghorn, W.L., and Fu, Jing-fan, 1989, "Allocation of Dimensional Tolerances for Multiple Loop Planar Mechanisms," *Journal of Mechanisms, Transmissions, and Automation in Design*, Vol 111, pp. 465-470.
7. Fogarasy, A.A. and Smith, M.R., 1998, "The Influence of Manufacturing Tolerances on the Kinematic Performance of Mechanisms," *Proc Instn Mech Engrs*, Vol 212 Part C, pp. 35-47.
8. Fortini, E. T., 1967, *Dimensioning for Interchangeable Manufacturing* Industrial Press New York, NY.
9. Hartenberg, R.S., and Denavit, J., 1964, *Kinematic Synthesis of Linkages* McGraw-Hill.
10. Huo, Hanqi, 1995, *New Tolerance Analysis Methods for Preliminary Design in Mechanical Assemblies*, Ph.D. Dissertation, Brigham Young University.
11. Knappe, L.F., 1963, "A Technique for Analyzing Mechanism Tolerances," *Machine Design*, April 25, pp. 155-157.

12. Lee, S.J., and Gilmore, B.J., 1991, "The Determination of the Probabilistic Properties of Velocities and Accelerations in Kinematic Chains with Uncertainty," *Journal of Mechanical Design*, vol 113, pp. 84-90.
13. Marler, Jaren D., 1988, *Nonlinear Tolerance Analysis Using the Direct Linearization Method*, Masters Thesis, Brigham Young University.
14. Ogot, M.M., and Gilmore, B.J., 1994, "A Kinematic Based Analysis for Tolerances Within Mechanical Assemblies," DE-Vol.69-1, *Advances in design Automation*, ASME Vol.1, pp. 237-249.
15. Sharfi, O.M.A., and Smith, M.R., 1983, "A Simple Method for the Allocation of Appropriate Tolerances and Clearances in Linkage Mechanisms," *Mechanism and Machine Theory*, Vol. 18, No 2, pp. 123-129.